COMPARISON OF SULFUR DIOXIDE AIR QUALITY DATA WITH THE PALSEM MODEL

A THESIS

Presented to
The Faculty of the Division of
Graduate Studies and Research

by

Diane M. H. Carlson

In Partial Fulfillment
of the Requirements for the Degree
Master of Science in Chemical Engineering

Georgia Institute of Technology

August, 1975

COMPARISON OF SULFUR DIOXIDE

AIR QUALITY DATA WITH THE PALSEM PROGRAM

Approved:

C. G. Justus, Chairman

David Orr, Jr.

R. G. Roper

Date Approved by Chairman: 8/8/75

ACKNOWLEDGMENTS

The author respectfully acknowledges the advice and guidance of Dr. C. G. Justus in the preparation and review of this work. She is also very grateful for the assistance of Dr. Clyde Orr, Jr., and Dr. R. G. Roper, who served on the Thesis Reading Committee. Much appreciation to Mr. Jim Motz of the Georgia Power Company and to Mr. Richard McRaine of Southern Services, Inc. for supplying technical assistance. Thanks also to Mrs. Myrna Thomas, Mr. Kenneth Miller, and Mr. John Stansfield for their assistance in the early preparation of this work.

A special thanks to my husband, Jim, who has been extremely encouraging, as usual, and to my grandfather, Mr. George A. Aebig, who sparked my initial interest in engineering.

This publication has been financed in part with Federal funds from the Environmental Protection Agency under fellowship number U-910358-01-0. The contents do not necessarily reflect the views and policies of the Environmental Protection Agency, nor does mention of trade names or commercial products constitute endorsement or recommendation for use.

TABLE OF CONTENTS

Page

ACKNOWLEDGMENTS. ii

LIST OF TABLES v

LIST OF FIGURES. vi

SUMMARY. vii

Chapter

I. INTRODUCTION. 1

Purpose and General Requirements of Dispersion Models
Purpose of Study
Factors Affecting Sulfur Dioxide Dispersion
Wind Speed and Direction
Turbulence
Inversions
The PALSEM Program
Input Characteristics
Computational Techniques
Output Characteristics
Description of the Air Sampling Network
Description of the Source

II. INSTRUMENTATION AND EQUIPMENT 28

Air Sampling Equipment
Meteorological Instrumentation

III. PROCEDURE 35

Data Acquisition
Data Preparation
PALSEM Runs

IV. RESULTS AND DISCUSSION OF RESULTS 41

V. CONCLUSIONS 58

VI. RECOMMENDATIONS 59

Appendix Page

A. PLUME RISE EQUATIONS. 63

B. GLOSSARY OF PALSEM INPUT VARIABLES. 66

C. STABILITY WIND ROSE TABULATIONS 70

D. EMISSION CALCULATIONS 78

E. NOMENCLATURE. 84

F. CONVERSION FACTORS. 87

G. EXAMPLE PALSEM OUTPUT 89

BIBLIOGRAPHY 110

LIST OF TABLES

Table		Page
1.	Stability Class by Temperature Difference.	9
2.	Source Data.	27
3.	Example Data Printout Sheet.	36
4.	Wind Speed Classes	37
5.	Frequency Distributions Measured and Predicted, TR 5, Y68.	42
6.	Frequency Distributions Measured and Predicted, TR 5, Y69.	43
7.	Frequency Distributions Measured and Predicted, TR 6, Y68.	44
8.	Frequency Distributions Measured and Predicted, TR 6, Y69.	45
9.	Cumulative Frequency Distributions, TR 5, Y68. . .	46
10.	Cumulative Frequency Distributions, TR 5, Y69. . .	47
11.	Cumulative Frequency Distributions, TR 6, Y68. . .	48
12.	Cumulative Frequency Distributions, TR 6, Y69. . .	49
13.	Summary of Observed and Predicted Statistics, TR 5, Y68.	50
14.	Summary of Observed and Predicted Statistics, TR 6, Y68.	51
15.	Boiler Emission Data, Y68.	80
16.	Boiler Emission Data, Y69.	81
17.	Frequency Distribution of Total Powerhouse Emission Output.	82

LIST OF FIGURES

Figure		Page
1.	Examples of Low Level Vertical Temperature Structure.	8
2.	Defining Geometry of x, y and angles θ_1 and θ_2 .	14
3.	Graphs of the AQDM and PALSEM Form Factors . . .	15
4.	Relative Locations of the Power Plant, the Weather Tower, TR 5, and TR 6.	25
5.	The Conductivity Cell.	31
6.	Sulfur Dioxide Monitor Flow Diagram.	33
7.	Cumulative Frequency Distributions, TR 5, Y68. .	52
8.	Cumulative Frequency Distributions, TR 5, Y69. .	53
9.	Cumulative Frequency Distributions, TR 6, Y68. .	54
10.	Cumulative Frequency Distributions, TR 6, Y69. .	55
11.	Cumulative Frequency of Total Powerhouse Emission Output.	83

SUMMARY

The introduction of air quality standards, hazardous air pollutant standards, and other ambient concentration limitations set to protect the public health and welfare has increased the need for pollutant transport and diffusion models, which are important in industrial expansion and land use planning. This work is a study of the Point, Area, and Line Source Emission Model (PALSEM), one of many dispersion models available to predict the effect of single and multiple emission sources on air quality.

Specifically, this study compares SO_2 air quality data collected downwind from a pulverized coal fired power plant with short term and hourly ground level concentrations computed using boiler operating data, meteorological information, and the PALSEM program. The boiler data and meteorological information are transformed to emission rates and stability wind roses for use in the PALSEM program.

The frequency distribution, annual arithmetic mean, geometric mean, geometric standard deviation, and 1 hour maximum are determined for the hourly air quality data and compared with the PALSEM predictions. Comparison of predicted and measured average concentrations and frequency distributions showed that the model did not accurately predict either one. Better correspondence of measured and predicted averages

would have been achieved by rotating the wind direction clockwise 22.5° (one sector).

The meteorological tower was approximately 1 mile perpendicular distance from the line of transport from source to receptor. Therefore, it is feasible that a direction shift occurred between the winds measured at the meteorological tower and the actual transport winds.

Since the power plant was NW of the monitoring sites, measured concentrations would be expected only during winds at or near a NW direction. While NW was the predominant direction for non-zero concentrations, measured values, some as high as 500 $\mu g/m^3$, occurred under virtually all wind directions. This indicates that either: (a) SO_2 reached the monitors from the power plant through some indirect route during periods of changing winds (in the model this could be considered a "self-induced background") or (b) that significant interference effects produced occasional high readings, even in the absence of SO_2 from the power plant plume.

Recommendations are given to allow the model to be calibrated in a way that minimizes the effects of problems encountered.

CHAPTER I

INTRODUCTION

Purpose and General Requirements of Dispersion Models

With the advent of air quality standards, hazardous air pollutant standards, and other ambient pollutant concentration limitations set to protect the public health and welfare, predictions of the degree of atmospheric diffusion, results of atmospheric reactions, and the fate of pollutants in general have become very important. Such predictions are very useful in land use planning.

This work is a study of the Point, Area, and Line Source Emission Model (PALSEM), one of many dispersion models available to predict the effect of single and multiple emission sources on air quality. This particular model is a modification of the Air Quality Display Model (AQDM) and may be used for point sources, line sources, or area sources. The accuracy and reliability of any model depends on the choice of variables and the suitability of the mathematical description for the physical situation. A model may work well in one physical situation but not in another.

A complete expression for the dispersion of material or pollutants released at a point must contain three

features [7]:

1. The shape of the distribution of concentration at any given time or downwind position, i.e., the manner in which the concentration varies across wind, vertically, and along wind (the latter being relevant only to the case of an instantaneous release of material).

2. The dimensions of the diffusing cloud in the cross wind, vertical, and along wind directions.

3. An expression of continuity or conservation of mass. Many diffusion models assume no material is lost by deposition, decomposition, or chemical reaction. This assumption results in conservative predictions which are most useful in protecting human health and welfare. If decay or reaction of a pollutant is desired, a half-life may be input into the PALSEM.

Purpose of Study

The purpose of this study is to compare short term and hourly ground level concentrations computed by the PALSEM program with sulfur dioxide air quality data collected near a pulverized coal fired power plant in 1968 and 1969. The study is concerned with the suitability, accuracy, and reliability of the PALSEM program in modeling this situation.

Factors Affecting Sulfur Dioxide Dispersion

Once sulfur dioxide is released into the atmosphere it is transported and diffused by the highly variable motions

of the atmosphere until it is removed by deposition, decomposition, chemical reaction, or animal, plant, or inanimate receptors. These atmospheric motions which may be highly variable in both space and time are typified by wind direction, wind speed, mechanical turbulence, and thermal turbulence.

Wind Direction and Speed

In the first thousand or so meters above the earth's surface the wind speed and direction are determined primarily by three forces: the force due to the horizontal pressure gradient, the coriolis force due to the earth's rotation, and the frictional force due to the nearness of the earth's surface [9].

The pressure gradient force is induced by horizontal pressure differences between any two points, greater pressure differences being associated with stronger winds. The pressure gradient alone would cause air to flow from regions of high to regions of low pressure. However, since the earth is turning beneath this flow an observer on the earth's surface in the Northern Hemisphere would notice an apparent turning of the flow to the right. This turning effect is the coriolis force. The net result of the pressure gradient and coriolis force in equilibrium is a flow that is parallel to the isobars with low pressure to the left of the direction of the motion in the Northern Hemisphere. The wind resulting from this balance is called the geostrophic wind. Winds in

the upper layer of the atmosphere approach geostrophic winds indicating that only pressure gradients and coriolis forces affect the flow [9].

Near the earth's surface a third force due to frictional drag becomes important. This force is caused by the difference in velocity of fluid layers flowing over a fixed surface. Such a fluid has a velocity of zero at the earth's surface or boundary with increasingly higher velocity as the distance from the surface increases. This force is due to molecular viscosity when flow is laminar or parallel to the surface [9]. In the atmosphere the role played by molecular viscosity near the surface of the earth is minor in comparison to that of turbulent or eddy viscosity. This is an apparent viscosity due to turbulent mixing that brings rapidly flowing air from aloft and transports slowly moving air near the surface to greater heights. In this way momentum is transferred from the lower atmosphere to the upper atmosphere. Thus turbulent viscosity gives rise to a frictional force which decreases with height and must be added to the pressure gradient and coriolis forces [9].

Friction not only reduces the wind speed near the surface but also changes the vector balance of the forces so that air near the surface moves at some angle to the geostrophic wind. In general the air flow at the earth's surface is directed to the left of the geostrophic flow at an angle that varies from about 15° by day over a smooth surface to 50° by

night over rough terrain. Above the surface the observed winds usually turn slowly in a clockwise manner so that the angle between the wind and the geostrophic wind gradually decreases with height until about 1000 meters above the ground where the observed wind is parallel and equal in magnitude to the geostrophic wind. The atmospheric layer below this level is substantially affected by surface friction while the atmospheric layer above this level is primarily influenced by upper level pressure forces and little affected by surface influences [9].

Even in the absence of turbulent mixing, the wind speed in any direction may change with height owing to the change with height of the large scale pressure distribution. This variation coupled with the smaller scale frictional effect results in a vertically varying wind structure [9].

Turbulence

Atmospheric turbulence is dependent upon three factors: the mechanical effects of objects protruding into the air stream which includes surface roughness, the vertical rate of increase of wind speed, and the vertical temperature structure of the atmosphere.

When the ground is smooth over a large area the air flow will tend to be laminar or streamlined. When the ground is rough the air must rise and fall over obstructions generating vertical turbulence. Horizontal turbulence is also generated by flow around objects. This mechanical turbulence

increases with higher wind speeds and, being generated at the surface, characteristically exhibits a decrease with height.

Turbulence causes not only transfer of momentum, but also transfer of heat. If air next to the ground is heated until it is warmer than the air above, a heat energy or thermal gradient will exist above the ground. A particle moving upward will have more thermal energy than a particle moving downward from above. Thermal energy is transferred from regions of high thermal energy to regions of low thermal energy. Thus there will be a net upward flux of heat due to turbulent motion [9].

The dispersive capability of the lower atmosphere is strongly influenced by the vertical temperature profile. This rate of temperature change with altitude is known as the temperature lapse rate. A positive lapse rate refers to a temperature decrease with altitude which is normally prevalent in the lower atmosphere. A negative lapse rate is a temperature increase with altitude and is associated with a temperature inversion. An isothermal lapse rate refers to no temperature change with altitude. When an atmospheric layer is completely mixed its temperature profile corresponds to a dry adiabatic lapse rate which has a temperature decrease with altitude of 5.4°F/1000 ft or 10°C/Km.

On a clear day with pronounced insolation (solar flux), lower layers of the atmosphere become warmed so that the air

temperature decreases with altitude at a rate greater than the dry adiabatic lapse rate. The atmosphere now has a superadiabatic lapse rate. On a clear night with light winds air layers adjacent to the ground are cooled by the earth's escaping long-wave radiation resulting in a vertical temperature profile that changes from positive to isothermal and then to a negative lapse rate. Several lapse rates are graphically depicted in Figure 1.

The temperature lapse rate is a good measure of the degree of both mechanical and thermal turbulence or instability in the atmosphere. Atmospheric stability may be referred to by a Pasquill stability class using the criteria in Table 1.

Inversions

Inversions are characterized by an increase in temperature with altitude. Such vertical stratification tends to inhibit turbulence and thus reduce atmospheric mixing.

At the earth's surface air generally flows radially outward from high to low pressure. This flow is compensated for by the sinking of the air in a high pressure system. When a layer of air sinks the temperature at the top of the layer increases more than the temperature at the bottom. If the layer sinks far enough a subsidence inversion will form.

Subsidence inversion layers are not normally based at the ground. These inversions are generally present in the eastern regions of the semipermanent oceanic high pressure

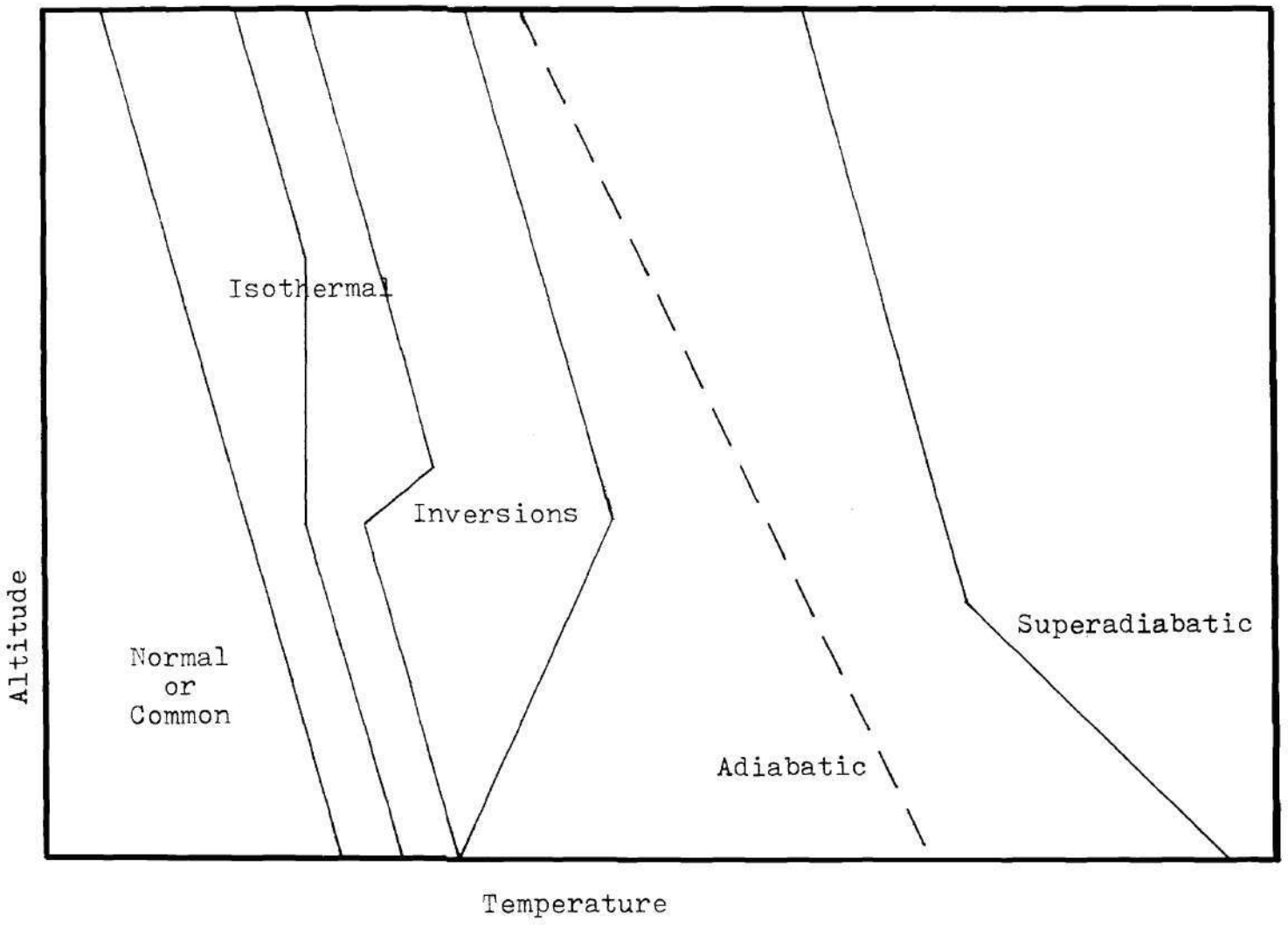

Figure 1. Examples of Low-Level Vertical Temperature Structure (9).

Table 1. Stability Class by Temperature Difference

Pasquill Class	Description	ΔT (°C)/100 M
A	Extremely Unstable	≤ -1.9
B	Unstable	-1.8 to -1.7
C	Slightly Unstable	-1.6 to -1.5
D	Neutral	-1.4 to -0.5
E	Slightly Stable	-0.4 to +1.4
F	Stable	+1.5 to +3.9
G	Extremely Stable	≥ +4.0

systems found at about 30°S and 30°N. In these locations they are reasonably permanent and stationary systems. Subsidence inversions are also found in high pressure systems associated with polar air masses which originate over the northern portion of the American and Asian continents. Since these are moving systems, no one locality is generally under the influence of the inversions for more than a few days [9].

A surface based radiation inversion is frequently associated with high pressure systems. This inversion is a nocturnal phenomena associated with clear nighttime skies and light winds. Both subsidence and radiation inversions may be wide spread, extending over areas ranging from tens of thousands to hundreds of thousands of square kilometers. The major difference between them is that the radiation inversion depends on the time of day, the nature of the surface and the local cloud cover, whereas subsidence inversion depends only on the large scale subsidence of the air mass [9].

High concentrations of sulfur oxides may occur particularly if an inversion traps the pollutant in a turbulent or unstable layer between an elevated source and ground level. The depth of this mixing layer, which may be affected by topography, limits the vertical dispersion of pollutants. The maximum mixing depth varies from day to day as well as from season to season.

The PALSEM Program

Input Characteristics

The PALSEM* is a modification of the AQDM*, which is based on a diffusion model developed by Martin and Tikvart [5,10]. The PALSEM is written in Fortran IV (level G) for a Univac 1108 or similar computer system. The main differences in input parameters between PALSEM and AQDM are:

1. The height of point and area sources may be input as well as heights of sampling stations and extra receptors.

2. The number of line sources and an array XLINE of line source emission data may be input. Array XLINE contains horizontal coordinates and height values for the end points of each line source as well as the total SO_2 and/or particulate emission rate in tons per day (TPD) for each line source.

3. A regional mean height may be input.

4. One wind speed, direction, and stability class may be input instead of an array of stability wind rose data. Also, stability classes A through G may be input instead of A through E which describe urban atmospheric stability.

5. Either the usual array of receptor grid locations at the height of the origin (RBASE) may be used or a set of receptors topographically varying in height may be input using the NAMELIST $HDATA Option. Either a circular (16 point compass) receptor grid or a plume centered receptor grid may be used if desired.

*Nomenclature is defined in Appendix E.

6. Plume rise may be predicted using the method of Holland, Moses and Carson, Concawe 1, Concawe 2, or Briggs. If desired no plume rise will be computed. An optional percentage increase or decrease in plume rise may be used to account for extra buoyancy as in cooling tower plumes or loss of plume rise due to building downwash. Plume rise equations are presented in Appendix A. Appendix E is a glossary of PALSEM Input variables.

Computational Techniques

Point and Area Sources. The PALSEM program uses a modified Martin-Tikvart [5] model for the computation of ground level concentration due to point and area sources. Area sources are treated as point sources displaced an appropriate distance upwind. If the wind direction assigned to a given 22.5° sector is, on the annual average, distributed uniformly over the sector, then the concentration X_o (in $\mu g/m^3$) due to a point source of emission strength Q (in $\mu g/sec$) is given at any point within the 22.5° sector by:

$$X_o(x,z) = (8Q/\sqrt{2}\ \pi^{3/2}\ xu\sigma_z)\ \{\exp[-(z-h)^2/2\sigma_z^2] + \exp[-(z+h)^2/2\sigma_z^2]\} \quad (1)$$

where x is the downwind distance, z is the receptor height (meters above the regional mean height above sea level,

RMHGT), h is the effective stack height (meters above RMHGT), u is the wind speed (m/sec), and σ_z is the vertical Gaussian standard deviation (in meters, given by a set of power law formulas built into the program). In order to avoid discontinuities in concentration from one directional sector to another, the AQDM program multiplies equation (1) by a parameter given by $[1 - (8y/\pi x)]$. The PALSEM program uses instead a multiplier function given by $\cos^2 4\theta_1$, where θ_1 is the angle whose tangent is y/x as illustrated in Figure 2. This factor varies from unity when $\theta_1 = 0$ to zero when $\theta_1 = 22.5°$. The $\cos^2 4\theta_1$ factor produces a more realistic bell shaped crosswind profile in the case of a single input wind direction (the AQDM crosswind factor is more-or-less triangular in shape). Note that the $\cos^2 4\theta_1$ factor is precisely complementary with the factor from the next adjacent sector, which is $\cos^2 4\theta_2 = \sin^2 4\theta_1$; that is, the sum of the factors from adjacent sectors in unity. Figure 3 shows a comparison between the $\cos^2 4\theta_1$ factor and the AQDM factor which can be expressed as $1 - 8 \tan \theta_1/\pi$. Note that the AQDM factor actually goes negative as θ_1 approaches 22.5°. For actual computation in the program $\cos^2 4\theta_1$ can be calculated without the use of trigonometric functions by the formula

$$\cos^2 4\theta_1 = [8\ C(C - 1) + 1]^2 \qquad (2)$$

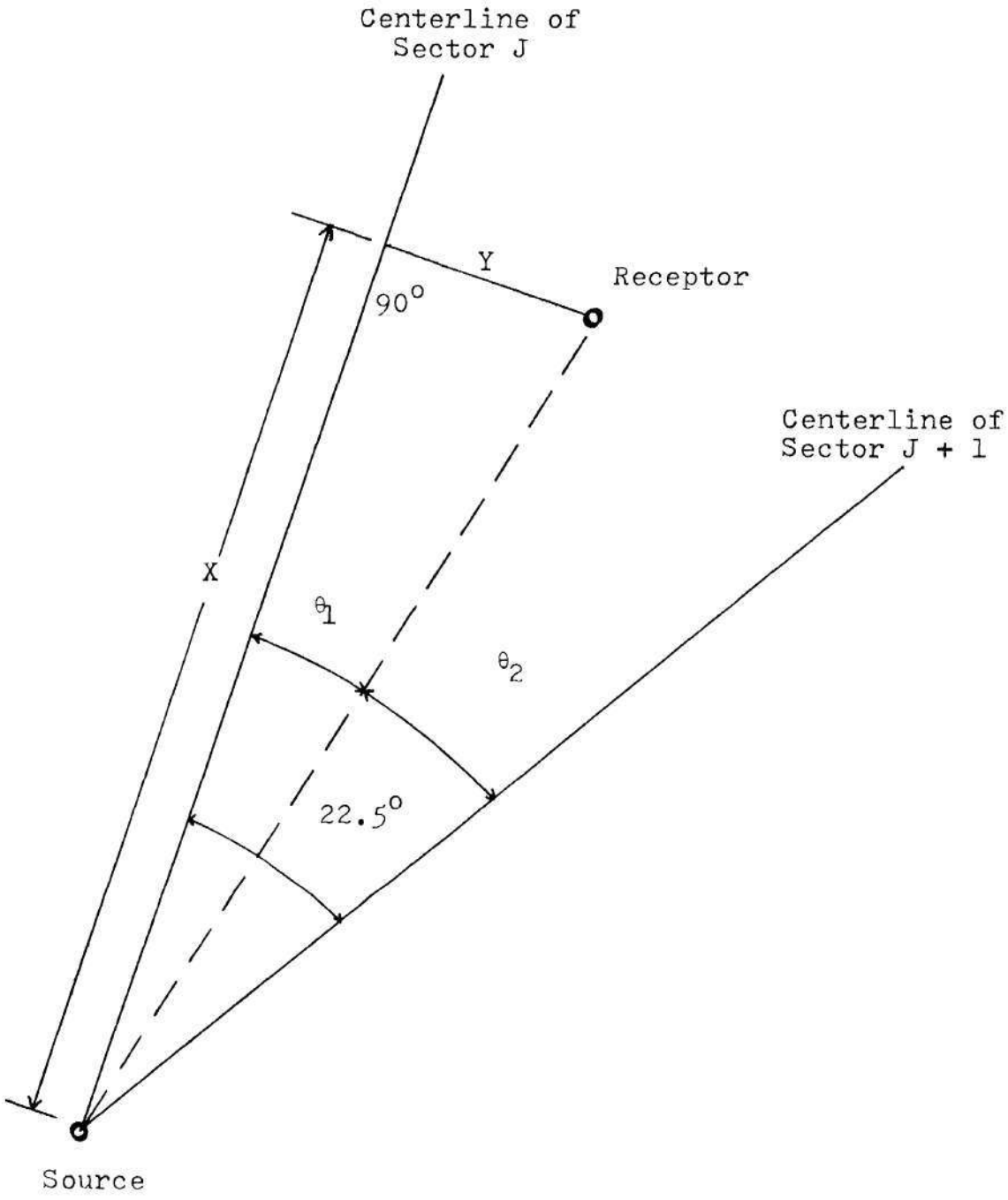

Figure 2. Defining Geometry of X, Y and Angles θ_1 and θ_2.

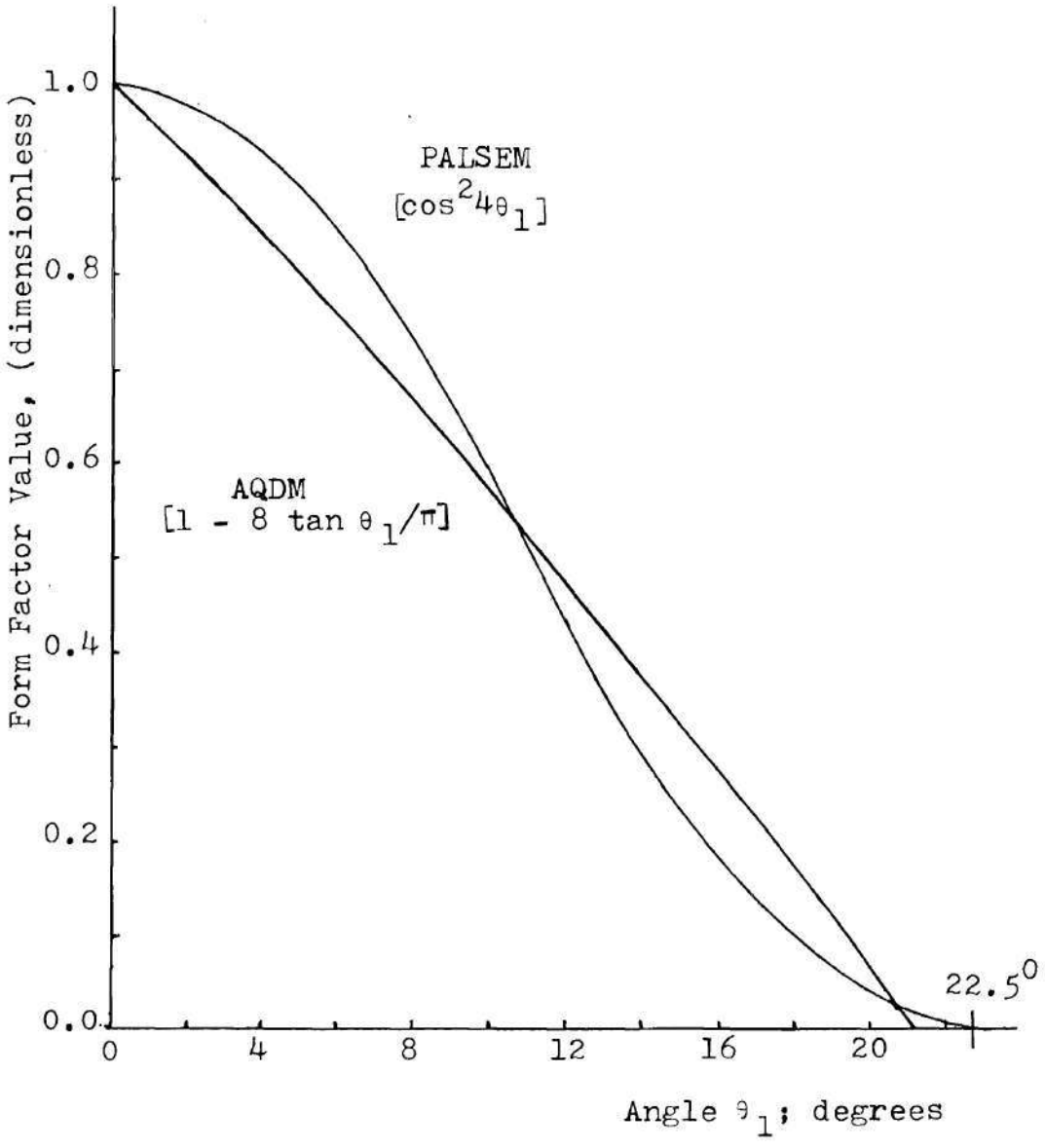

Figure 3. Graphs of the AQDM and PALSEM Form Factors

where C^2 is $\cos^2\theta_1$ and can be computed from $C^2 = x^2/(x^2 + y^2)$. The concentration χ is computed from equation (1) by

$$\chi = \chi_o \cos^2 4\theta_1 \tag{3}$$

The application of equation (3) does not continue for all downwind distances x because of plume reflection which takes place both at the RMHGT plane and the RMHGT + DPTHMX plane. As with the Martin-Tikvart model, equation 1 applies up to a downwind distance $x = x_L$ at which $\sigma_z = 0.47$ L, where L is the value of DPTHMX. For down wind distances $x \geq 2x_L$ the relation

$$\chi = 8\ Q \cos^2 4\theta_1/\pi\ L\ ux \tag{4}$$

is used and between x_L and $2x_L$ linear interpolation is used between equation (4) evaluated at $2x_L$ and equation (3) evaluated at x_L. The point source relative concentrations x/Q are computed in the program by a subroutine RELCO which has as input parameters x, y, z, h, u, L and the stability class index s for calculation of σ_z.

Line Sources

Downwind concentrations due to line sources are computed by calculating a numerical approximation to the integral

$$\chi = \int_{o}^{S} R\, q\, ds \qquad (5)$$

where R is the relative concentration function computed by subroutine RELCO, the same as used for point sources, q is the line source strength (μg/m sec), and ds is an element of path length along the line source of total length S. Since the relative concentration subroutine RELCO is dependent on both source and receptor heights, the height of the line source can be made to vary from one end to the other. Only straight line sources of constant strength q along their length are allowed by the program, although more complex curved lines could be approximated by a sequence of straight line segments.

The integral expression equation (5) is computed by a Richardson extrapolation technique, a successive approximation method which, at each step, is equivalent to a Simpson's rule integral approximation, and which subdivides the line into twice as many segments on each successive step. The successive approximations to the integral continue until convergence (to within 2%) occurs or until the line has been subdivided into a maximum number of segments, the value of which can be set by the input parameter NSEG. The starting side of the line integration is always from the end which would produce the maximum relative concentration and the summation for each successive approximation is terminated

when the subroutine RELCO produces a relative concentration R less than 10^{-3} times the sum of the previously computed relative concentrations along the line, i.e. when $R_n < 10^{-3} \Sigma$ where Σ is the sum on i from 1 to n - 1 of R_i.

Receptor Grids. Four types of receptor grids may be used to evaluate concentrations:

1. A rectangular grid.
2. A circular grid.
3. A set of plume centered points within the plume of a selected source.
4. An array of receptor points whose x,y,z coordinates are input via the optional NAMELIST $HDATA

A circular grid which was used in this study is centered at the position RBASE and has points oriented along the 16 point compass directions from RBASE at the radius values given by the array XCOORD. There may be from 1 to 9 radius values. The circular grid may also have multiple vertical levels.

The optional input array NAMELIST $HDATA is available to account for irregular terrain or topography. The x,y, and z coordinates of each receptor point are input separately. This allows receptor heights above sea level (Km) to be read from topographic maps and input into the program. The topography for the dispersion study region is reasonably flat so this option was not used.

Hourly Concentration Distributions. A new feature of

the PALSEM program is the ability to evaluate distributions of hourly concentrations from stability wind rose data. For these computations each occurrence of wind speed, wind direction, and atmospheric stability is assumed to represent one particular hourly condition which is possible at various times throughout the year. At each receptor location hourly concentrations are computed for each speed direction and stability combination. Next the probability value in the stability wind rose is assigned as the probability of observing that particular hourly concentration. Finally for each receptor point the probabilities of observing hourly concentrations within certain ranges are evaluated by summing the probabilities of all the concentrations actually computed as lying within certain ranges. The hourly concentration ranges built into the program in micrograms per cubic meter are 0-50, 50-100, 100-200, 200-400, 400-800, and 800-9999. These concentration ranges may be altered to any six other ranges. From the frequency of the hourly concentrations occurring in these ranges of values it is usually possible to compute such factors as maximum hourly concentration once per year occurrence which may be different from the largest computed hourly concentration.

Boundary Layer Winds. Height variations of winds in the boundary layer are accounted for by first evaluating the plume rise, $\Delta h(x)$, at the instantaneous downwind position x and then correcting wind velocity as follows:

$$V(\Delta h) = V_o(\Delta h/Z_o)^n \qquad (6)$$

V_o is the speed value for the particular speed class under consideration and Z_o is the height of the anemometer at which the wind rose data were measured. The exponent n varies with stability class. Values of n used in the program are 0.1 (class A), 0.15 (class B), 0.2 (class C), 0.25 (classes D through G). If Z_o equals zero in the program then $V(\Delta h)$ is taken to be the same as V_o. In the program no attempt is made to compensate for changes in the wind direction in the boundary layer.

Reactive Pollutants. For reactive pollutants, a half-life in the atmosphere (T in hours = HALF) may be specified. If the nonreactive pollutant concentration is χ_n, then the reactive pollutant concentration χ_r is computed by:

$$\chi_r = \chi_n \exp(-0.69315\ x/(uT)) \qquad (7)$$

where x is the downwind distance (m), u is the wind speed (MPS), and T is converted to seconds in the program. For point sources the wind speed u is the wind speed at the plume rise height (if a height varying wind speed is used). For area sources, u is the wind speed at the height of the area source. For line sources, u is the wind speed at the height of the midpoint of the line, and x is the downwind distance between the midpoint of the line and the receptor.

Maximum Concentrations Computed from Hourly Distributions. When hourly concentration distributions are evaluated, maximum concentrations (once per year recurrence) are computed for averaging times of one hour (and any three times specified by SO2AVG and PARAVG). From the distribution of *hourly concentrations* due to meteorological variabilities, a lognormal distribution is evaluated by least squares fit. The geometric standard deviation (GSD), σ_m, is evaluated for the best fit lognormal distribution. The hourly concentration which would be exceeded with the probability of 1/8766 is also evaluated from the best fit lognormal distribution. Revised GSDs due to combined meteorological and source emission variability are evaluated by computing σ_m and the GSD, σ_e, of source emission variability. The resultant GSD, σ_t, due to both meteorological and emission variations is computed by:

$$\sigma_T = \exp[(\ell n\ \sigma_m)^2 + (\ell n\ \sigma_e)^2] \qquad (8)$$

Revised one hour maximum concentrations are computed from the new lognormal distribution specified by the σ_t. Maximum concentrations once per year recurrence are evaluated for averaging times other than one hour by a power law interpolation between the one hour maximum concentration determined from σ_t and the annual average concentration.

Palsem Output

The PALSEM output is essentially the same as for the AQDM and consists of listings of the point and area source input, the line source input, the meteorological data input, the regression parameters, and/or correlation data for the calibration curve, the receptor concentration data, the optional statistical data for selected receptors and the source contribution data for either five selected receptors or the five maximum concentration receptors, and optional punch output of the receptor concentration data for plotting purposes. Heights of the sources and the receptors are listed in kilometers. The horizontal receptor coordinates but not the receptor heights are punched on the optional punch output.

A new type of output not in the AQDM is the hourly concentration distribution. For each pollutant and each receptor, the frequencies in percent are listed for the occurrence of hourly concentrations within each of six concentration intervals. From these distribution data a maximum hourly concentration once per year recurrence can be calculated.

For the five sites for which source contribution data are evaluated, a directional distribution of average hourly concentrations is also output. This distribution shows, for each of the sixteen different wind directions, the annual average hourly concentrations at each of the five

sites or receptors for all speed and stability conditions which occurred during the year.

Description of the Air Sampling Network

An air sampling network was set up to collect SO_2 concentration data downwind of a pulverized coal fired power plant. Information collected by the network includes wind velocity, wind direction, temperature lapse rate, and particulate and SO_2 concentrations at ground level. Particulates were measured with high volume samplers over 24 hour periods. Sulfur dioxide was measured with a recording SO_2 analyzer measuring instantaneous and half-hour average SO_2 concentrations at ground level. Lead peroxide candles and dust fall jars were also used around the emission source to determine the best location for more sophisticated sampling devices.

Data from the recording SO_2 analyzers covering the period from January, 1968, through August, 1969, was used in the PALSEM study. At the beginning of this time interval a Davis SO_2 analyzer housed in sampling trailer 5 (TR 5) was located 4.55 miles (5.713 Km) southeast of the power plant. In May, 1968, TR 6 and a second Davis analyzer were placed in operation. This analyzer was located 4.55 miles (7.322 Km) southeast of the power plant. Sequential samplers employing the West Gaeke method on a long term basis (24 hours) were also tried during the study.

These samplers exhibited many problems. For instance, the sampler would not maintain a constant air flow, condensation occurred in the lines leading from the impinger to the pump, the timer malfunctioned, and impinger solution evaporated. Problems associated with the analytical technique included dye instability and staining of colorimeter valves. Due to the many problems experienced with the West Gaeke method, the Davis analyzer results were deemed more useful in the air quality study.

A 300 foot weather tower, initially used in August, 1967, collected weather data such as the wind speed, wind direction, and temperature change with altitude. In addition a sigma computer continuously recorded the changes in the wind direction by degrees. All of the variables from the weather tower as well as readings from the SO_2 analyzers were tabulated manually from recorder charts onto data sheets.

The PALSEM study uses the recorded weather data and SO_2 analyzer data as well as hourly boiler operating parameters and fuel information. The locations of the sampling trailers and the weather tower relative to the power plant are shown in Figure 4.

Description of the Source

The primary source of SO_2 within 40 miles of the sampling trailers is a 1540 MW fossil fuel power plant.

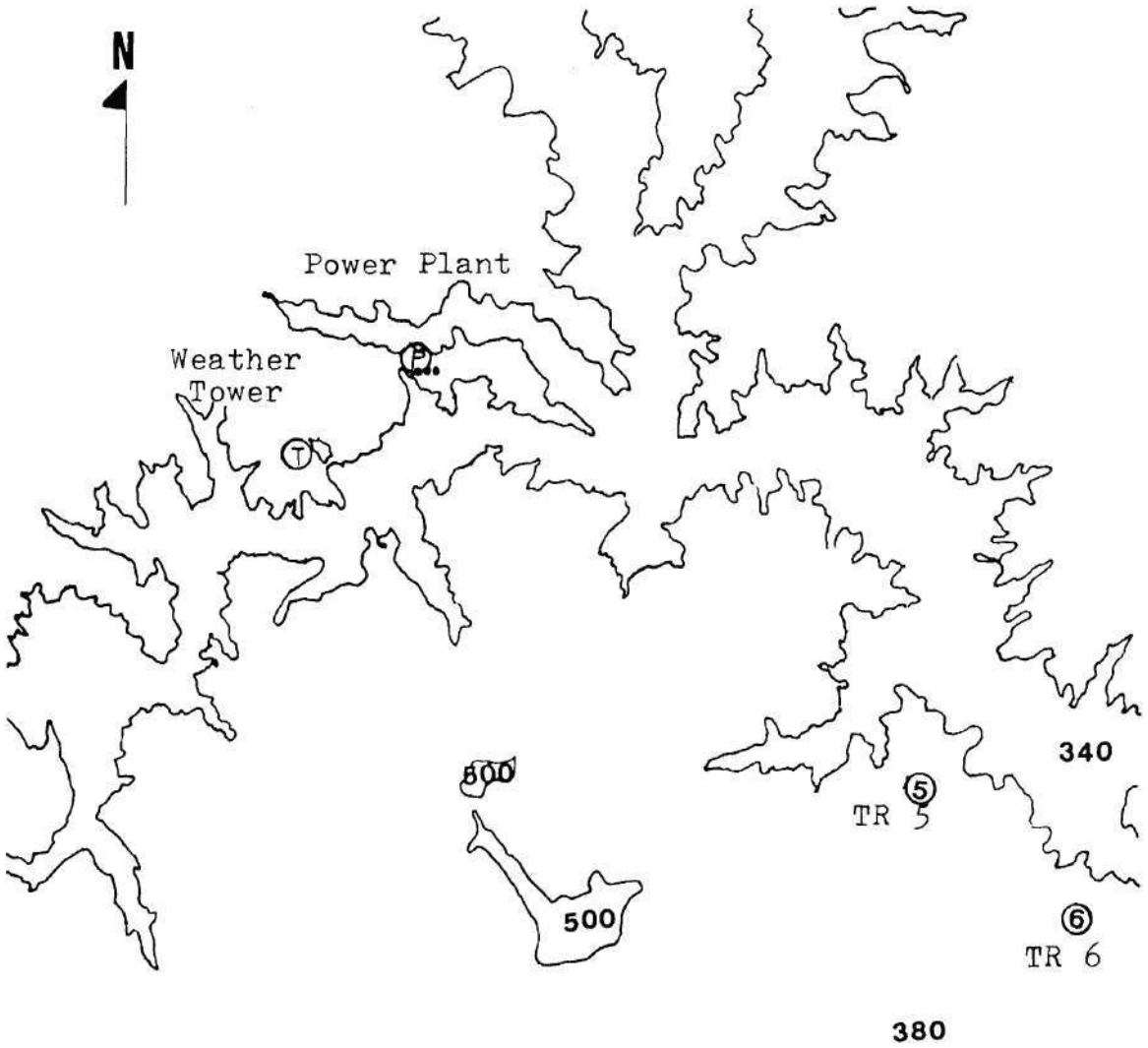

Scale: 1" = 1 mile
Elevations above sea level
are in boldface type

Figure 4. Relative Locations of the Power Plant, the Weather Tower, TR 5, and TR 6

During the study interval of 1968-69 four pulverized coal fired boilers were operated at the plant site. Unit 1, rated at 250 MW, and Unit 2, rated at 319 MW, were both operating at the beginning of the PALSEM study interval. Both units utilized electrostatic precipitators to remove particulates from stack exhaust gases. The precipitators operated at 97.6 and 98.5% efficiency, respectively. Boiler unit 3, rated at 480.7 MW or 3,380,219 pounds of steam per hour, was initially operated in June of 1968. Unit 4 rated at 490 MW or 3,563,400 pounds of steam per hour, initially started up in May, 1969. Electrostatic precipitators operating at 98.2 and 97.3% efficiency were used with these units. Source data such as amount of fuel burned, ash content, sulfur content, heat content, stack exhaust gas temperature, stack diameter, and stack height are presented in Table 2.

Table 2. Source Data

	Unit 1	Unit 2	Unit 3	Unit 4
Rated Output, PPH steam	1,750,000	2,246,000	3,382,219	3,563,400
Rated Output, MW	250	319	480.7	490
% Excess Air	18	20	18	18
Fuel Consumption, at Rated Output, PPH	194,200	245,835	372,000	N.A.
Type of Fuel	PC	PC	PC	PC
% Ash	12	12	12	12
% Sulfur	0.9-3.0	0.9-3.0	0.9-3.0	0.9-3.0
Heat Content, Btu/hr	12,000	12,000	12,000	12,000
Stack Diameter, Ft	16	15	21	21
M	4.88	4.57	6.4	6.4
Stack Height, Ft	300	350	500	500
M	91.44	106.7	152.4	152.4
Stack Exhaust Gas Temperature, °F	270	270	270	270

CHAPTER II

INSTRUMENTATION AND EQUIPMENT

Air Sampling Equipment

Prior to the study interval an Instrument Development Company SO_2 analyzer was operated to obtain ambient air concentration data. Operation of the IDC analyzer was abandoned due to excessive downtime and continuous maintenance requirements. Davis Model 70A1 analyzers operating during this same time period operated more reliably and required little maintenance. One undesirable feature of the Davis analyzers was that they were not specific for SO_2. This was not considered to be much of a problem since the location of the sampler was such that interfering gases were not likely to be present. Interfering gases include chlorine, oxides of nitrogen, ammonia, and CO_2. According to studies of continuous sulfur dioxide monitors [7] the Davis analyzer had:

1. The fastest response time (1.5 minutes with others having up to 26.5 minutes).

2. The highest collection efficiency (99.94% with others ranging to 98.7%).

3. A zero drift in 24 hours (0.2% of the chart with others ranging from 0.0% to 1.3%).

4. Sensitivity to the lowest level of sulfur dioxide (0.01 ppm with others as high as 0.03 ppm).

5. The highest interference from chlorine, ammonia, and CO_2 (1 ppm of chlorine gave 0.39 ppm sulfur dioxide interference).

The Davis SO_2 analyzer operates on the principal of electrical conductance caused by ionization of dissolved material. This is accomplished by measuring resistance of a sample and water mixture passing over a pair of electrodes. Errors due to polarization, i.e., the changes of the composition of the solution adjacent to the electrodes are eliminated by employing alternating current [1].

The Davis monitor is designed for continuous readings. This is accomplished by recirculating the water. All effluent from the special analyzing cell is continuously purged to an ion exchange reservoir where mono-bed deionization takes place. The sensitivity of the monitor depends on the total number of ions formed and is affected by the rate of the flow of the sample with respect to the rate of the flow of water since these determine the concentration of the sample in the water [1].

The Davis SO_2 analyzers were calibrated using Teflon permeation tubes. The rate of permeation of liquid SO_2 through the walls of the tubes was measured by chemical analysis (Barium perchlorate titration of bubbler sampler) to check the calibration supplied by the manufacturer. With

information on the permeation rate and the air flow rate of the analyzer the permeation tube was inserted into a holder and used to calibrate the analyzer. Three different permeation tubes in the range of 25%, 50%, and 75% of scale on the SO_2 analyzer were desirable to check for linearity [1].

An ac measuring circuit and a dc indicating portion were employed. A constant source of alternating current was maintained for the special analyzing cell. Output from this cell was rectified and sent through the measuring circuit. During normal operation the circuit path was through the active electrodes. When the efficiency of the mono-bed resin was checked, the circuit path was through sample free water check electrodes [1].

The primary element of the measuring system is a conductivity cell which is fabricated from clear, resistant, insoluble plastic. The air sample passes through a rotometer and enters the cell at point A shown in Figure 5. The ion free water enters the cell at point B. The water passes over water check electrodes. Then both the sample and water are mixed together in the cell chamber. From the chamber the solution passes between active electrodes where the electrical resistance is measured. After being analyzed the solution leaves the cell at point C where it is sent through a suction device back to an ion exchange reservoir. The water check electrodes are positioned upstream from the mixing of the sample water so that if the ion filters are

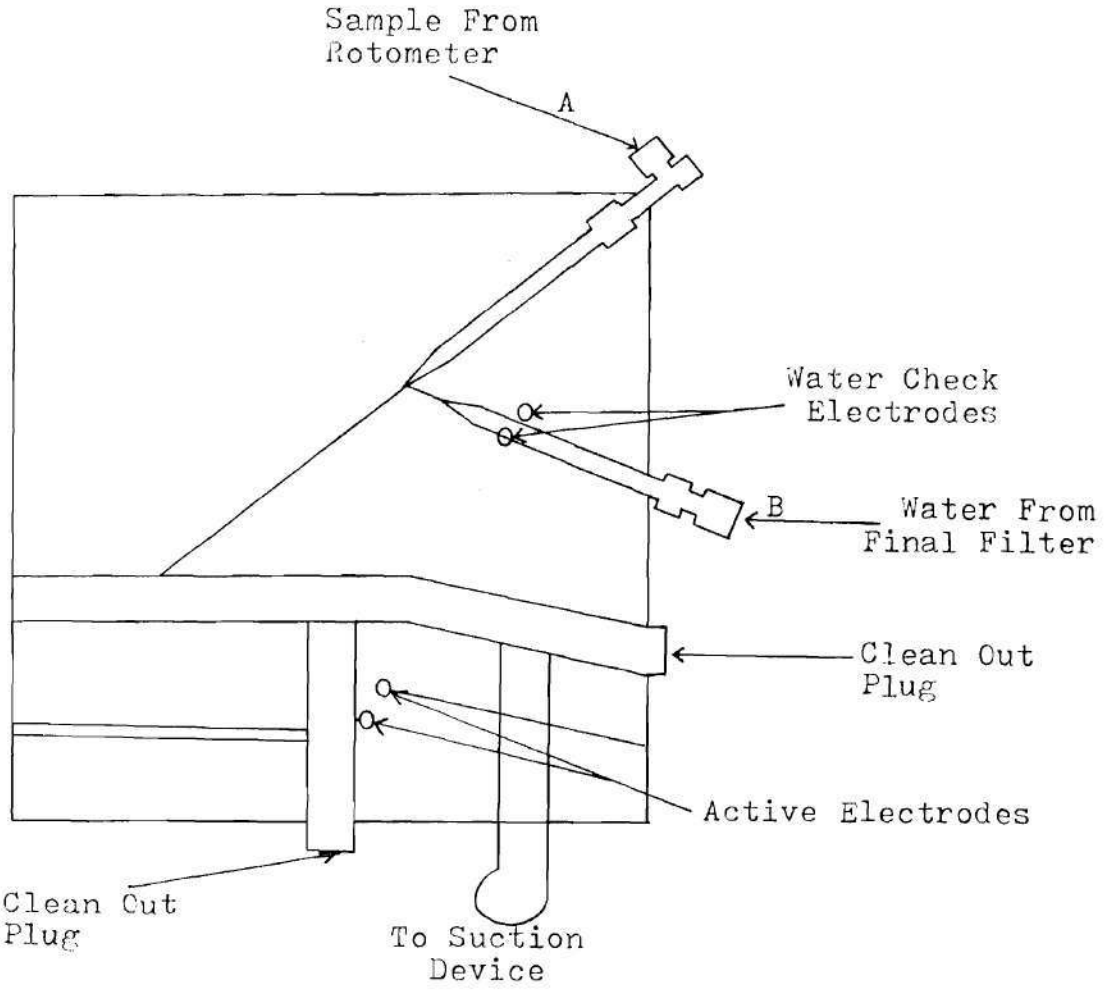

Figure 5. The Conductivity Cell

functioning properly correct recorder or meter indication should be near zero. If the electrodes are turned or if the cell is replaced the instrument must be recalibrated at zero.

The ion exchange unit, shown in the flow diagram in Figure 6, is both a reservoir and an ion exchange chamber. The chamber contains Amberlite MB-3, a self-indicating mixture of cation and anion exchange resins. As the efficiency of the resin decreases, the color changes from bluish green to brown. Water from the ion exchange chamber is filtered a second time through a final ion filter. Any ions which have been picked up by the water while flowing through the middle components of the valve and water meter are removed. All tubing after the final ion filter is nonmetallic.

The SO_2 absorber is a plastic chamber containing water and ion exchange resin which absorbs SO_2 in the sample gas. It is connected in such a way that periodically the sample passes through it before the sample reaches the cell. This gives a reading of the sample gas with the sulfur dioxide removed.

The CO_2 absorber is a plastic chamber containing soda lime which removes CO_2 from the sample gas. It is connected so that the sample periodically passes through it and the SO_2 absorber before entering the cell. This gives a reading of sample gas with the SO_2 and CO_2 removed.

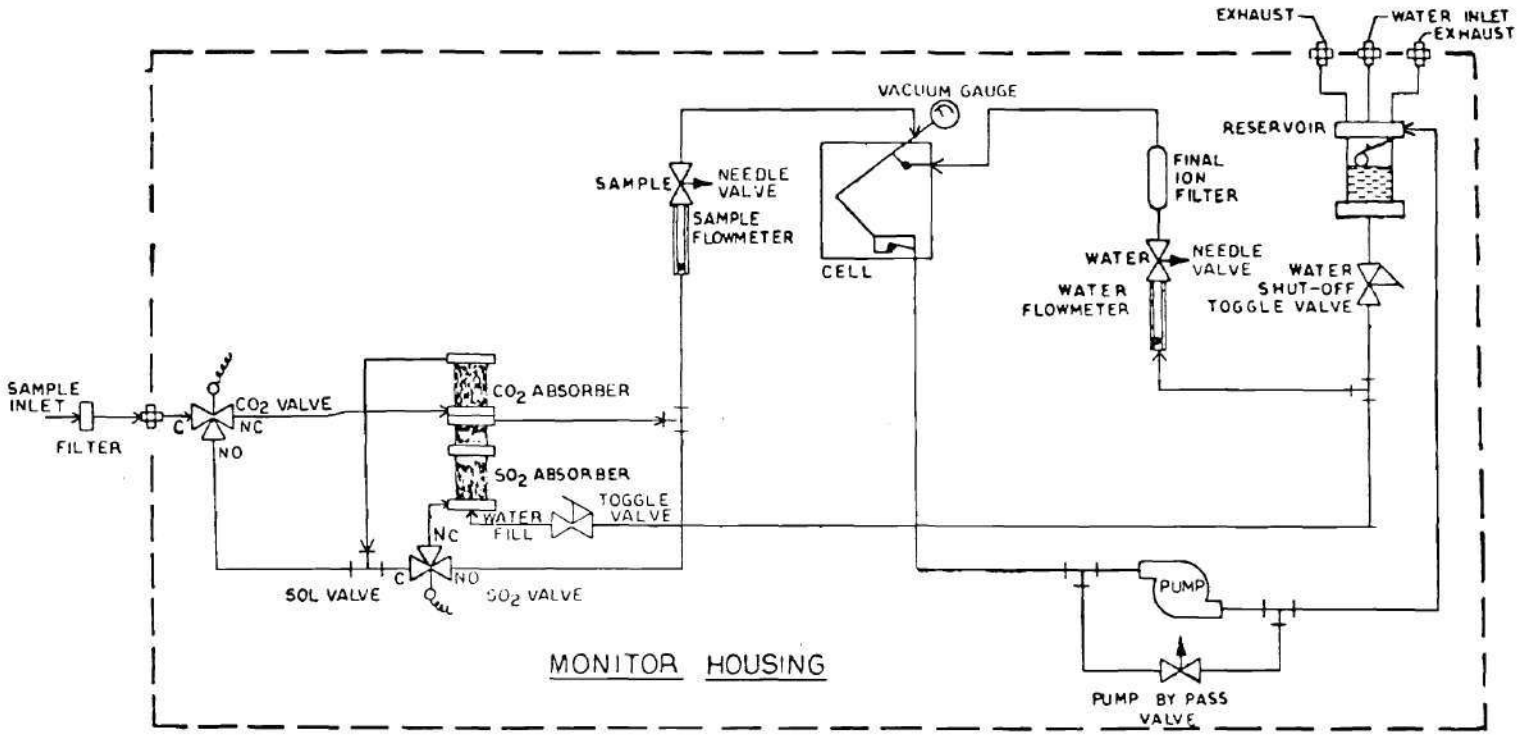

Figure 6. Sulfur Dioxide Monitor Diagram

Meteorological Instrumentation

Wind speed, wind direction, and temperature gradient information were collected on a 300 foot weather tower situated on a hill. Wind speed and wind direction sensors were located at the 300 foot level and temperature sensors were at the 33, 100, and 300 foot levels. The sensor at the 33 foot level was used for ambient temperature measurement and the sensors at 100 and 300 foot levels recorded the differences in temperature between these heights. This temperature difference was used to determine the atmospheric stability. Weather data was recorded continuously at the tower. Later the wind direction and wind speed were manually tabulated for every hour. Wind direction variance and temperature lapse rate were tabulated for every half hour.

CHAPTER III

PROCEDURE

Data Acquisition

During the ambient sampling period from 1966 through 1969, data were taken from several sources and recorded on master data sheets from which IBM cards were punched.

In construction of the data sheets, the wind direction and wind speed were tabulated for every hour. Wind direction sigma, and temperature lapse rates were tabulated for every half hour. Plant MW outputs were recorded every hour for each unit two hours before and after any readings were detected by the SO_2 analyzers. A weekly composite fuel sample was routinely analyzed and the sulfur analysis from that composite sample was tabulated for the same hours as plant output. Peak and half-hour average SO_2 concentrations were tabulated in ppm.

Listings of the IBM data printout from January, 1968, through August, 1969, were used in the PALSEM study. An example data printout sheet follows in Table 3. The data were divided into two one-year intervals, January, 1968, through December, 1968, and September, 1968, through August, 1969. These intervals are referred to as Y68 and Y69, respectively.

DATA NO	DATA SYSTEM	HOUR	WIND SPEED	WIND DIRECTION	HORIZONTAL DEG. SIG.	VERTICAL DT/1000	UNIT 1	UNIT 2	UNIT 3	UNIT 4	TOTAL MEG	PCT S IN COAL	SO2 DAVIS 1/2 HR AVG	FACTOR
77	3/ 4/69	5	9	158	0/ 0	-10.0	273	0	0	0	273		TR5 / TR6 / TR7 /	
78	3/ 4/69	6	9	158	0/ 0	-12.5	273	0	0	0	273		TR5 / TR6 / TR7 /	
79	3/ 4/69	7	13	135	0/ 0	-12.5	278	0	0	0	278		TR5 / TR6 / TR7 /	
80	3/ 4/69	8	16	135	0/ 0	-14.0	285	0	0	0	285	1.5	TR5 / TR60.0 /0.04 TR7 /	4.3
81	3/ 4/69	9	15	135	0/ 0	-14.5	288	0	0	0	288	1.5	TR5 .10/.11 TR60.19/0.21 TR7 /	4.3
82	3/ 4/69	10	15	135	0/ 0	-13.5	289	0	0	0	289	1.5	TR5 .06/.03 TR60.02/0.12 TR7 /	4.3
83	3/ 4/69	11	25	158	0/ 0	-12.5	286	0	0	0	286	1.5	TR5 / TR60.0 /0.03 TR7 /	
84	3/ 4/69	12	23	158	0/ 0	-11.0	258	0	0	0	258		TR5 / TR6 / TR7 /	
85	3/ 4/69	13	23	158	0/ 0	-9.5	249	0	0	0	249		TR5 / TR6 / TR7 /	
86	3/ 4/69	14	17	158	0/ 0	-7.5	249	0	0	0	249	1.5	TR5 .0 /.03 TR60.0 /0.03 TR7 /	
87	3/ 4/69	15	17	158	0/ 0	-6.0	253	0	0	0	253	1.5	TR5 .06/.06 TR60.05/0.02 TR7 /	3.8
88	3/ 4/69	16	17	158	0/ 0	-5.0	286	0	0	0	286	1.5	TR5 .08/.03 TR60.03/0.07 TR7 /	4.3
89	3/ 4/69	17	17	158	0/ 0	-4.5	287	0	0	0	287	1.5	TR5 .0 /.01 TR60.0 /0.01 TR7 /	
90	3/ 4/69	18	16	158	0/ 0	-1.0	289	0	0	0	289	1.5	TR5 .02/.03 TR60.0 /0.02 TR7 /	
91	3/ 4/69	19	3	0	0/ 0	30.0							TR5 / TR6 / TR7 /	
92	3/ 4/69	20	18	180	0/ 0	4.0	290	0	0	0	290	1.5	TR5 .04/.03 TR60.04/0.03 TR7 /	4.3

Table 3. Example Data Printout Sheet

Data Preparation

For each one year period punched data from the IBM data listing were used to compute a stability wind rose, source emissions, and ambient concentration statistical information which are tabulated in Appendices C and D and Chapter IV, respectively.

The stability wind rose was constructed according to the National Climatic Center STAR format using Pasquill stability classes A through G. The procedure was first to determine the stability class for each hour using the measured temperature lapse rate and Table 1. Next the wind direction (direction the wind was blowing from) was determined for each hour using a 16 point compass.

For each stability class-wind direction situation the concurring wind speeds were separated into classes one through six according to Table 4.

Table 4. Wind Speed Classes

Class	Speed, MPS	Speed, Mi/Hr
1	< 1.80	< 4.0
2	1.80 - 3.34	4.0 - 7.5
3	3.34 - 5.40	7.5 - 12
4	5.40 - 8.49	12 - 19
5	8.49 - 11.06	19 - 24.75
6	> 11.06	> 24.75

Finally the frequency of occurrence of each speed class in each of the 16 wind directions for the seven stability classes was tabulated. The annual average SO_2 emission rate ($\bar{Q}$) in TPD and a typical average exhaust gas velocity (V) in MPS were computed for each unit using hourly values of output MW, %S, and the exhaust gas temperature, % ash, % combustibles, and inner stack diameter as described in Appendix D. The GSD (1 hour averaging time) of total SO_2 emissions for all four (4) units, σ_e, was also determined for use in the meteorology-emission computation in PALSEM.

Ambient concentration measurements were converted from two half-hour readings in ppm to one hourly reading in $\mu g/m^3$ at 289°K (60.5°F) and 981 mb, the annual average temperature and pressure. A concentration frequency distribution was constructed from data for each sampling trailer site. Arithmetic and geometric means as well as arithmetic standard deviations and 1 hour average geometric standard deviations (GSDs) were computed. Maximum hourly concentrations were also determined. The 24 hour average GSD at each sampling trailer site was required for the PALSEM statistical output. The 24 hour σ_g can be calculated from the 1 hour σ_g using the following logarithmic distribution relationship [4]:

$$\sigma_{gb} = \sigma_{ga}^{V^{0.5}} \tag{9}$$

where

$$V = \frac{\ln (t_{tot}/t_b)}{\ln (t_{tot}/t_a)} \tag{10}$$

For the conversion from a 1 hour to a 24 hour averaging time let

$$t_{tot} = 8766 \text{ hours/year}$$

$$t_a = 1 \text{ hour}$$

$$t_b = 24 \text{ hours}$$

therefore

$$V = \frac{\ln (8766/24)}{\ln (8766/1)} = 0.64994 \tag{11}$$

$$\sigma_{gb} = \sigma_{ga}^{0.8062} \tag{12}$$

For instance if σ_g is 2.11 for a 1 hour averaging time

$$\sigma_{gb} = 2.11^{0.8062} = 1.82 \tag{13}$$

for a 24 hour averaging time.

PALSEM Runs

A total of four situations were modeled with each year

of data. The first three runs used a background of 0.0 $\mu g/m^3$ and assumed (1) no plume rise, (2) plume rise predicted by Briggs, and (3) plume rise predicted by Holland's method. The average annual temperature (289°K), pressure (981 mb), and mixing depth (970 m) from climatological summaries were used for all runs. The fourth run utilized a background level of 0.01 ppm or 26.5 $\mu g/m^3$ and Briggs' plume rise method. The 26.5 $\mu g/m^3$ background level was chosen to illustrate the effect of background levels on the PALSEM. Background levels were not measured during the sampling interval, however they do exist. The Briggs' plume rise method was chosen since it reasonably models large power plant plumes.

Average concentrations, frequency distributions, and other concentration statistics computed by the PALSEM runs were then compared to ambient concentration statistics.

CHAPTER IV

RESULTS AND DISCUSSION OF RESULTS

Tabular summaries of the eight computer runs are presented in Tables 5 through 14. In addition, the computer printout for Y69 using Briggs' plume rise is included as an example in Appendix G.

In Tables 5 through 8 the measured SO_2 frequency distribution, which appears lognormal in Figures 7 through 10, indicates that approximately 60% of the measurements at TR 5 and 66% of the measurements at TR 6 are between 50 and 200 $\mu g/m^3$. The PALSEM frequency distribution predicts 68 to 69% of the readings at TR 5 and 84 to 88% of the readings at TR 6 will be less than 50 $\mu g/m^3$. Only 14 to 24% of the readings at TR 5 and 5 to 9% at TR 6 are expected to be between 50 and 200 $\mu g/m^3$. The discrepancy can be explained by noting that the measured annual arithmetic means (AMS) exceed the predicted AMS by a factor of 2 to 5 and recalling that the PALSEM frequency distribution depends on the stability wind rose and concentrations computed with the Gaussian diffusion model. If the AM is low then the frequency distribution shows a high percentage of low concentrations.

The effect of adding a background level is to shift the frequency distribution to higher concentration levels,

Table 5. Frequency Distributions Measured and Predicted at TR 5, Y68

Concentration Range $\mu g/m^3$	Observed by Davis Analyzers	Predicted by PALSEM			
		Briggs	Hollands	No Rise	Briggs W/BKGR
0-50	18.34	69.27	65.61	62.58	68.16
50-100	33.40	5.25	5.25	5.57	2.07
100-200	32.62	17.04	14.97	14.65	11.78
200-400	12.74	8.44	11.78	10.99	17.99
400-800	1.93	0.00	0.95	2.87	0.00
800-9999	.96	0.00	1.43	3.34	0.00

Table 6. Frequency Distributions Measured and Predicted at TR 5, Y69

Concentration Range $\mu g/m^3$	Observed by Davis Analyzers	Predicted by PALSEM			
		Briggs	Hollands	No Rise	Briggs w/BKGR
0-50	22.70	88.04	85.44	83.88	86.73
50-100	28.11	0.65	0.13	0.13	1.82
100-200	31.53	7.02	8.45	6.89	2.73
200-400	13.69	4.16	4.16	4.29	8.58
400-800	2.70	0.13	1.82	3.38	0.13
800-9999	1.26	0.00	0.00	1.43	0.00

Table 7. Frequency Distributions Measured and Predicted at TR 6, Y68.

Concentration Range $\mu g/m^3$	Observed by Davis Analyzers	Predicted by PALSEM			
		Briggs	Hollands	No Rise	Briggs w/BKGR
0-50	22.59	68.16	65.13	62.58	68.16
50-100	34.07	13.22	12.58	12.10	6.37
100-200	32.59	10.51	10.83	10.51	17.36
200-400	7.78	8.12	9.24	8.76	8.12
400-800	2.96	0.00	2.23	2.71	0.00
800-9999	0.00	0.00	0.00	3.34	0.00

Table 8. Frequency Distributions Measured and Predicted at TR 6, Y69.

Concentration Range $\mu g/m^3$	Observed by Davis Analyzers	Predicted by PALSEM			
		Briggs	Hollands	No Rise	Briggs w/BKGR
0-50	26.44	88.04	85.44	83.88	86.73
50-100	32.22	3.12	2.60	2.60	1.95
100-200	29.25	5.59	5.59	4.81	7.15
200-400	10.33	3.25	5.33	5.33	4.03
400-800	1.75	0.00	1.04	2.08	.13
800-9999	0.00	0.00	0.00	1.30	0.00

Table 9. Cumulative Frequency Distributions, TR 5, Y68.

Concentration $\mu g/m^3$	Observed	Predicted by PALSEM			
		Briggs	Hollands	No Rise	Briggs w/BKGR
50	18.34	69.27	65.61	62.58	68.16
100	51.74	74.52	70.86	68.15	70.23
200	84.36	91.56	85.83	82.80	82.01
400	97.10	100.00	97.61	93.79	100.00
800	99.03		98.56	96.66	
9999	99.99		99.99	100.00	

Table 10. Cumulative Frequency Distributions
TR 5, Y69.

Concentration $\mu g/m^3$	Observed	Predicted by PALSEM			
		Briggs	Hollands	No Rise	Briggs w/BKGR
50	22.70	88.04	85.44	83.88	86.73
100	50.81	88.69	85.57	84.01	88.55
200	82.34	95.71	94.02	90.90	91.28
400	96.03	99.87	98.18	95.19	99.86
800	98.73	100.00	100.00	98.57	99.99
9999	99.99			100.00	

Table 11. Cumulative Frequency Distributions
TR 6, Y68.

Concentration $\mu g/m^3$	Observed	Predicted by PALSEM			
		Briggs	Hollands	No Rise	Briggs w/BKGR
50	22.59	68.16	65.13	62.58	68.16
100	56.66	81.38	77.71	74.68	74.53
200	89.25	91.89	88.54	85.19	91.89
400	97.03	100.00	97.78	93.95	100.00
800	99.99		100.00	96.66	
9999				100.00	

Table 12. Cumulative Frequency Distributions
TR 6, Y69.

Concentration $\mu g/m^3$	Observed	Predicted by PALSEM			
		Briggs	Hollands	No Rise	Briggs w/BKGR
50	26.44	88.04	85.44	83.88	86.73
100	58.66	91.16	88.04	86.48	88.68
200	87.91	96.75	93.63	91.29	95.83
400	98.24	100.00	98.96	96.62	99.86
800	99.99		100.00	98.70	99.99
9999				100.00	

Table 13. Summary of Observed and Predicted Statistics at TR 5, Y68 and Y69

Concentration Statistics	Observed by Davis Analyzers		Wind Rose Emission Prediction		Larsen Statistics	
	Y68	Y69	Y68	Y69	Y68	Y69
AM	124	131			60 B 81 H 136 N 86 BB	25 B 38 H 60 N 51 BB
GM	91	90			44 B 59 H 100 N 63 BB	17 B 26 H 42 N 36 BB
σ_g 1 hour averaging time	2.2	2.37	2.48 B 3.01 H 2.74 N 2.92 BB	2.88 B 3.18 H 4.01 N 2.85 BB	2.20 B 2.20 H 2.20 N 2.20 BB	2.36 B 2.36 H 2.36 N 2.36 BB
1 Hour Max	930	1178	953 B 1924 H 1534 N 1643 BB	802 B 1161 H 2273 N 829 BB	892 B 1200 H 2025 N 1286 BB	457 B 690 H 1106 N 944 BB
Observations per site	518	555				

B Briggs
H Hollands
N No Plume Rise
BB Briggs with Background

Table 14. Summary of Observed and Predicted Statistics at TR 6, Y68 and Y69.

Concentration Statistics	Observed by Davis Analyzers		Wind Rose Emission Prediction		Larsen Statistics	
	Y68	Y69	Y68	Y69	Y68	Y69
AM	108	107			47 B 64 H 110 N 73 BB	20 B 30 H 47 N 46 BB
GM	81	82			35 B 48 H 84 N 55 BB	15 B 23 H 37 N 36 BB
σ_g 1 hour averaging time	2.11	2.06	2.45 B 2.50 H 2.75 N 2.43 BB	3.01 B 3.29 H 3.96 N 2.81 BB	2.10 B 2.10 H 2.10 N 2.10 BB	2.06 B 2.06 H 2.06 N 2.06 BB
1 hour Max	694	537	941 B 1073 H 1561 N 925 BB	895 B 1258 H 2201 N 802 BB	600 B 824 H 1423 N 942 BB	241 B 360 H 574 N 562 BB
Observations per site	270	571				

B Briggs
H Hollands
N No Plume Rise
BB Briggs with Background

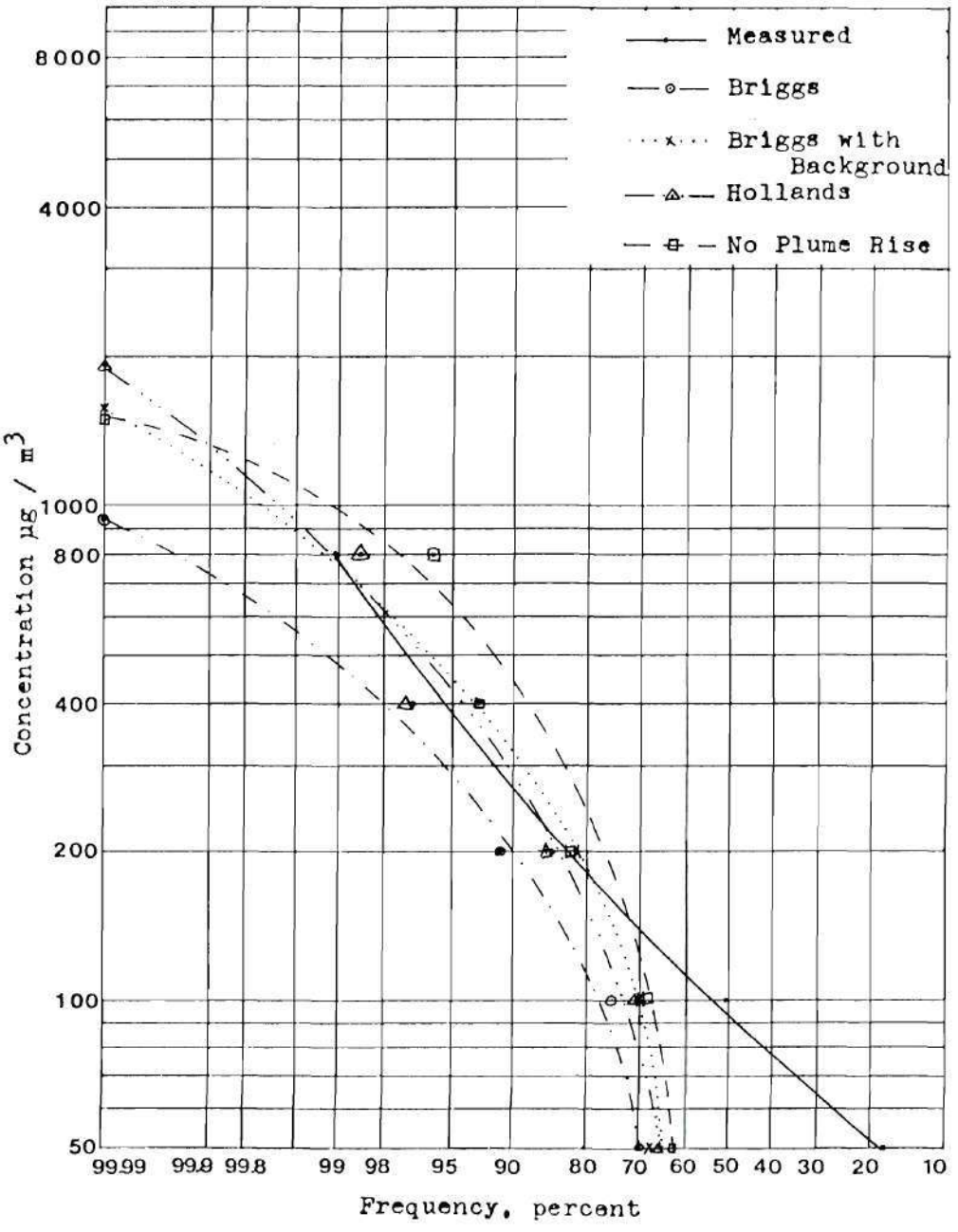

Figure 7. Cumulative Frequency Distributions, TR 5, Y68

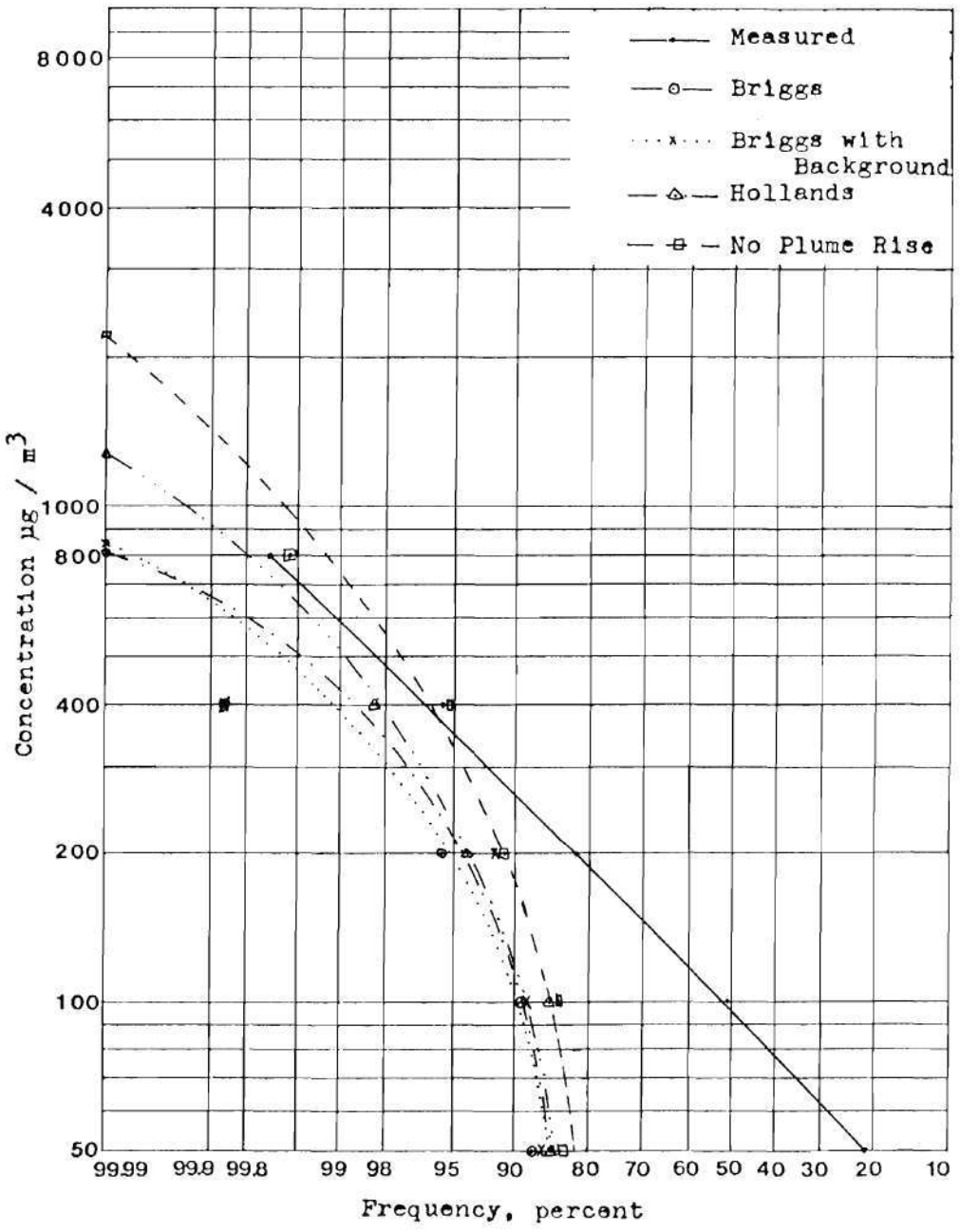

Figure 8. Cumulative Frequency Distributions, TR 5, Y69

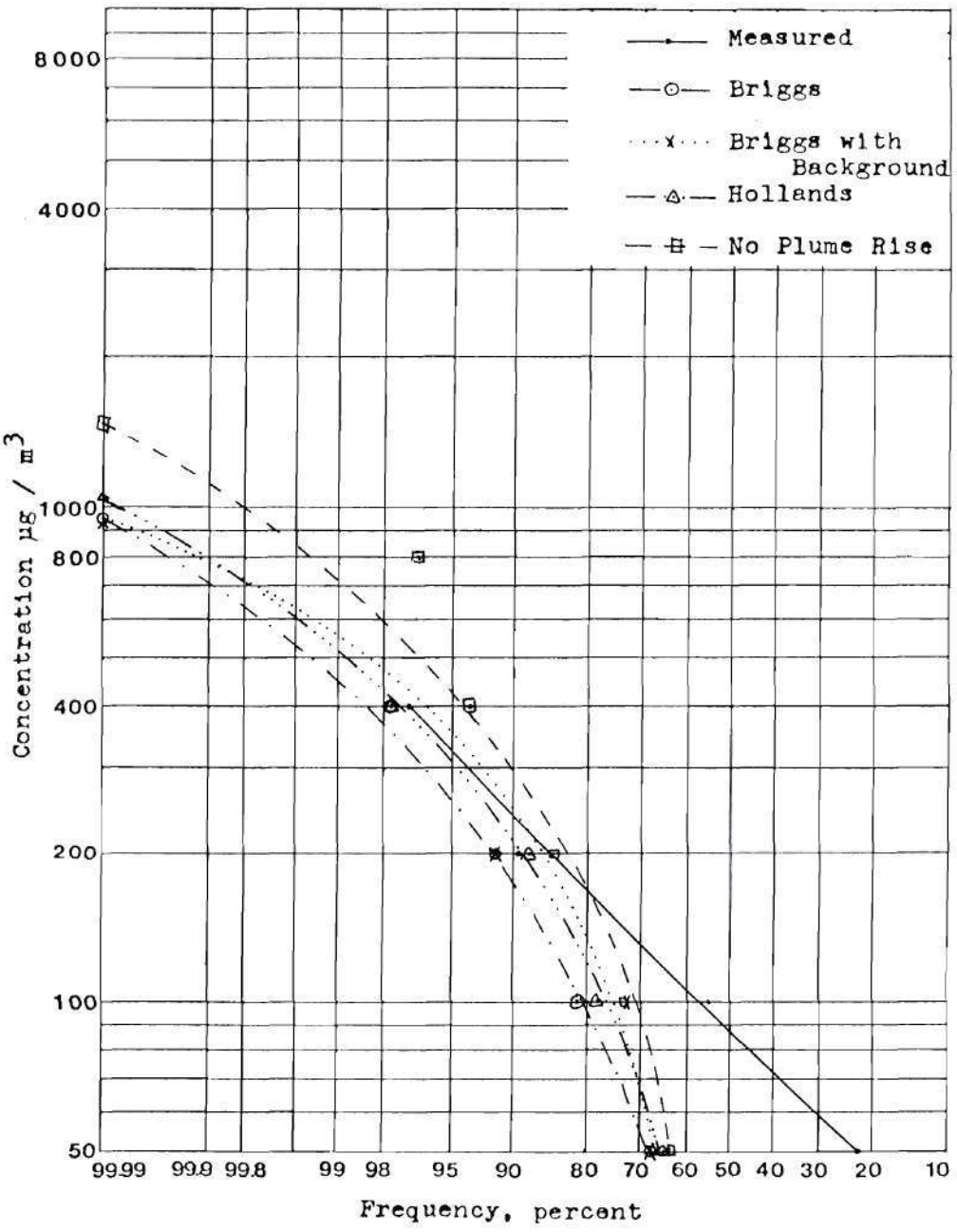

Figure 9. Cumulative Frequency Distribution, TR 6, Y68

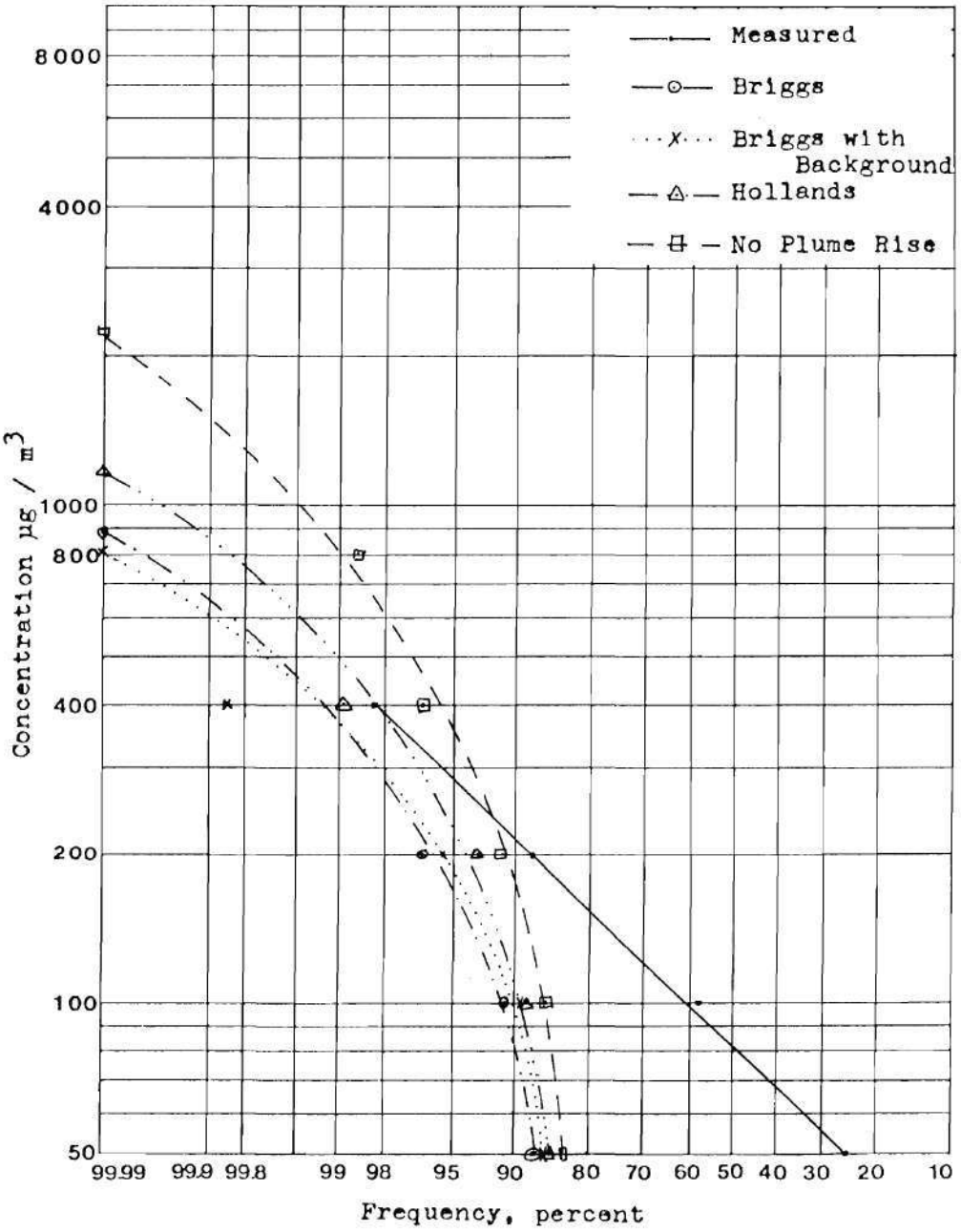

Figure 10. Cumulative Frequency Distribution, TR 6, Y69

increase the AM by a constant, and increase the predicted maximum hourly concentration. The effect on the predicted concentration GSD depends on the magnitude of the background and may be either an increase or a decrease.

The ratio of AM_{obs} to AM_{pred} ranges from 1.8 to 2.4 for Y68 and from 2.33 to 5.35 for Y69. This is partially due to a higher SO_2 emission rate of 261.4 TPD in Y68 as compared to 250.7 TPD in Y69. Also the average height of the stacks used in Y68 was less than that of the four stacks used in Y69. The lower height of emission results in a higher maximum ground level concentration and may result in higher concentrations at TR 5 and TR 6. The influence of 3 hours of F and G stability in Y68 and eight hours of F and G stability in Y69 which may increase concentration levels due to poor mixing is not apparent.

Discrepancies between the observed and computed concentrations may also be due to the Davis analyzers which are nonspecific for SO_2. Although CO_2 was removed in the analyzer to reduce interferences, other substances may cause higher than actual readings. Ammonia decreases ionization and lowers the readings. Calibration of the analyzers with permeation tubes which may vary in diffusion rate depending on conditions of storage and use may further decrease reliability of the measurements. Also the wind direction at the tower may differ from that reaching the sampling site. This is caused by the variation of wind

direction with height described in Chapter I or by a channelling effect due to the nearby lake. The wind direction is critical for short term concentration studies especially when related to specific receptor sites [3].

CHAPTER V

CONCLUSIONS

Comparison of the PALSEM program output with SO_2 concentrations measured at two sampling sites located downwind of a fossil fuel power plant suggests that either the model, as used, does not describe the physical situation or that data used for the comparison are inaccurate or insufficient. Specific results of this comparison follow:

1. The predicted AM varies from 20 to 50% of the observed AM.

2. The PALSEM frequency distribution predicts 68 to 69% of the readings at TR 5 and 84 to 88% of the readings at TR 6 will be less than 50 $\mu g/m^3$. Ambient measurements indicate that only 14 to 20% of the readings at TR 5 and 5 to 9% at TR 6 are in this concentration range. Most of the ambient measurements are between 50 and 200 $\mu g/m^3$.

3. Comparisons of the predicted 1 hour maximums with observed one hour maximums are not meaningful due to lack of sufficient sampling data.

CHAPTER VI

RECOMMENDATIONS

Discrepancies between the model predictions and measured data could be due in part to SO_2 monitor interferences, to the effect of wind direction on receptor concentration measurements, and/or to background levels.

Ambient air data used in this study were collected by continuous Davis analyzers which despite their operating reliability are nonspecific for SO_2 and are affected by several interfering gases. During the years of 1968 and 1969 when the data were collected, this analytical method was probably one of the best available. Now that more specific and reliable sampling techniques are available, it is recommended that the PALSEM program, using emission data from all sources in the area, be compared with these more precise methods. Along with more precise sampling methods, a more reliable calibration method should be utilized. Permeation tubes such as used in this study have met with several criticisms concerning constancy of the diffusion rate under storage and calibration conditions. Devices are now available for use in calibration which allow much more control over mixing specific quantities of SO_2 with certain amounts of air.

Wind blowing over the terrain near the source may change direction from place to place. The meteorological tower is located approximately 1 mile from a line joining the power plant and the monitoring sites. Thus a wind reported as NW at the weather tower may actually be a NNW transport wind. This occurrence is indicated by the computed average concentrations in Appendix G, which show that values at receptors 14 and 30 (corresponding to NNW winds) agree better with average measured concentrations than with those computed at receptors 15 and 31 (corresponding to NW winds). It is suggested that the wind rose be rotated one complete sector (22.5°) clockwise to approximate the wind rose of actual transport winds. Concentrations and frequency distributions predicted by PALSEM could then be compared with ambient concentration statistics to determine the effect of wind direction.

Background concentrations may be estimated from ambient concentration data by assuming that the average measured concentration for all wind directions except N, NNW, and NW, which are in the general direction of the source, are either: (a) "self-induced" contributions to the background, i.e., SO_2 which reaches the monitors from the power plant through an indirect route during periods of changing wind directions, or (b) contributions from other sources and interfering substances. Thus a background, either real, "self-induced," or due to interference effects could be

computed for each receptor location.

The computed average background level may be used with the SO_2 calibration parameters (slope = 1, intercept = 0) to compute concentrations. Alternatively, the computed background may be used with annual arithmetic means at TR 5 and TR 6 to calibrate the model and then compute concentrations. The resulting predicted concentrations and frequency distributions may then be compared with ambient data statistics. Definite improvement in the comparison of observed and model predicted average concentrations is expected. It is not clear, however, how much improvement could be expected in the comparison of observed and predicted concentration frequency distributions. Therefore the frequency distribution calculation features of the PALSEM model must be considered unproven until the results of these recommendations are investigated.

APPENDICES

APPENDIX A

PLUME RISE EQUATIONS

The Holland plume rise formula [12] with an adjustment factor for stability effect (1.4 - 0.1 L) and a height factor F(x) for variation during the rise phase, is given by

$$\Delta h = (1.5\ V\ d + 0.04\ Q_H)(1.4 - 0.1\ L)\ F(x)/U \qquad (14)$$

where V is the exit velocity (MPS), d is the exit diameter (m), Q_H is the heat flux (Cal/sec), L is the stability class (1 = extremely unstable to 7 = very stable), U is the wind speed, MPS. F is given by

$$F(x) = (x/10h_s)^{2/3} \qquad (15)$$

where x is downwind distance and h_s is stack height. For unstable cases (L < 4) the Moses and Carson plume rise is

$$\Delta h = (3.47\ V\ d + 10.53\ Q_H^{1/2})\ F(x)/U \qquad (16)$$

while for neutral cases (L = 4) it is given by

$$\Delta h = (0.35\ V\ d + 5.41\ Q_H^{1/2})\ F(x)/U \qquad (17)$$

and for stable cases (L > 4) it is given by

$$\Delta h = (-1.04\ V\ d + 4.58\ Q_H^{1/2})\ F(x)/U \qquad (18)$$

The CONCAWE #1 formula is

$$\Delta h = 2.58\ Q_H^{0.58}\ F(x)/U^{0.70} \qquad (19)$$

and the CONCAWE #2 formula is

$$\Delta h = 5.53\ Q_H^{1/2}\ F(x)/U^{0.75} \qquad (20)$$

The Briggs formulas [11] are given in terms of general conditional situations, as follows:

(a) if U < 1 and L > 4

$$\Delta h = \text{MINIMUM of } \Delta h_1 \text{ and } \Delta h_2 \text{ where} \qquad (21)$$

$$\Delta h_1 = 7.82\ Q_H^{0.25}/\Delta\theta^{0.375}$$

$$\Delta h_2 = 2.98\ (Q_H/U\ \Delta\theta)^{1/3}$$

and $\Delta\theta = 0.015$ (or 0.037 if L > 5)

(b) if U $\geq$ 1 and L > 4

$$\Delta h = 0.538\ Q_H^{1/3}\ x^{2/3}/U \quad (\text{if } x < x^*) \qquad (22)$$

or

$$\Delta h = 2.96(Q_H/U\Delta\theta)^{1/3} \quad (\text{if } x \geq x^*) \tag{23}$$

where $x^* = 12.7\ U/\Delta\theta^{1/2}$ and $\Delta\theta$ is the same as above

(c) if $Q_H \leq 5000$ and $L \leq 4$

$$\Delta h = 0.538\ Q_H^{1/3}\ x^{2/3}/U \quad \text{if } x < 3x_s \tag{24}$$

or

$$\Delta h = 0.784\ Q_H^{0.6}\ h_s^{0.4}/U \quad \text{if } x \geq 3x_s$$

$$\text{where } x_s = 18\ Q_H^{0.4} \quad \text{if } h_s > 304.8\text{m} \tag{25}$$

$$\text{or } x_s = 0.585\ Q_H^{0.4} h_s^{0.6} \quad \text{if } h_s < 304.8\text{m}$$

(d) if $Q_H > 5000$ and $L \leq 4$

$$\Delta h = 0.538\ Q_H^{1/3}\ x^{2/3}/U \quad (\text{if } x < 10h_s) \tag{26}$$

or

$$\Delta h = 2.5\ Q_H^{1/3}\ h_s^{2/3}/U \quad (\text{if } x \geq 10h_s) \tag{27}$$

APPENDIX B

GLOSSARY OF PALSEM INPUT VARIABLES

PALSEM Additions to AQDM	Name	Description
	BACKGR	Array including background concentrations ($\mu g/m^3$) for SO_2 and particulates.
*	DELTA X	Spacing between columns of rectangular grid receptors (Km).
*	DELTA Y	Spacing between rows of rectangular grid receptors (Km).
*	DELTA Z	Vertical spacing between grid receptor levels (Km).
*	DMXE	Mixing depth for E stability plus F and G if used (m).
	DPTHMX	Average afternoon mixing depth (m).
	$END	Control card indicating that input data cards have been read.
*	HALF	Half-life for SO_2 and particulates (hr).
*	$HDATA	Control card indicating that all following data is to be input.
	IADD	Number of non-grid receptors.
	ICØNP	Receptor numbers for particulate receptors selected for source contribution output.
	ICØNS	Receptor numbers for SO_2 receptors selected for source contribution output.
*	ICOORD	Number of X coordinates for plume centered receptors or radius values for circular grid receptors.

PALSEM Additions to AQDM	Name	Description
*	ICROSS	Option for cross wind plume width.
	IFLAG	Flag to indicate which calibration option is to be used.
*	IHRC	Concentration range limits for hourly concentration distributions ($\mu g/m^3$).
	INCRX	Number of columns of receptor grids.
	INCRY	Number of rows of receptor grids.
*	INCRZ	Number of vertical levels of receptor grids.
	$INDATA	Control card indicating that all following data is to be input.
	IPUNCH	Flag to indicate whether or not cards for map plotting are to be punched.
	ISTATP	Receptor numbers for particulate receptors selected for statistical output.
	ISTATS	Receptor numbers for SO_2 receptors selected for statistical output.
*	NLINE	Number of line sources.
	NPART	Number of particulate sampling stations to be used in calibration.
	NPOLUT	Flag to indicate which pollutants are to be used.
*	NPLREQ	Number of plume rise equation to be used.
*	NRECEP	Number of receptors used with $HDATA.
*	NSAZ	Wind direction index
*	NSEG	Maximum number of segments a line will be divided into during iterative numerical integration.

PALSEM Additions to AQDM	Name	Description
	NSEL5	Flag to indicate receptor selection for source contribution output.
	NSEL12	Flag to indicate whether or not statistics are to be output.
	NSO2	Number of SO_2 measuring stations to be used in calibration.
	NSORCE	Number of sources input
*	NSORGN	Source number for origin of plume centered receptors
*	NSC	Number of stability classes to be used.
*	NSSC	Stability index for single wind condition
*	NSSP	Speed class for single wind condition.
	PA	Ambient pressure (mb).
	PARAVG	Averaging times for particulate statistical output (hr).
	PARCAL	Regression line constants for particulates
	PAROB	Array including particulate sampling station locations and measurements.
	PLUME	Array including stack exit velocity (MPS), stack diameter (m), and stack exhaust temperature (°K), for each source.
	RBASE	Coordinates of grid receptor origin.
*	RECEPT	Receptor locations for $HDATA.
*	RMHGT	Regional mean height above sea level (Km).
	SGDP	Particulate standard geometric deviations for statistical output receptors.

PALSEM Additions to AQDM	Name	Description
	SGDS	SO_2 standard geometric deviations for statistical output receptors.
*	SGM	Geometric standard deviation for emission variability which affects hourly distributions.
	SO2AVG	Averaging times for SO_2 statistical output.
	SO2CAL	Regression line constants for SO_2.
	SO2OB	Array including SO_2 sampling station locations and measurements.
	SORCE	Array including source location (Km), area (Km^2), emission rate (TPD), and physical stack height (Km), for each source.
	TA	Ambient temperature, °K.
*	WNDFRF	Wind rose for F stability.
*	WNDFRG	Wind rose for G stability.
	WNDFRQ	Stability wind rose for A through E stability.
*	WSPD	Actual wind speed for a single wind condition (MPS).
*	XCOORD	X coordinates for plume centered receptors or radius values for circular grid (Km).
*	XLINE	Array of coordinates of each end of a line source (Km) and SO_2 and particulate emission rate (TPD).
	XRECEP	Locations of non-grid receptors (Km).
*	ZO	Height of anemometer above ground (m).

APPENDIX C

STABILITY WIND ROSE TABULATIONS

A stability wind rose for Y68 utilizing 628 hourly observations is tabulated in the following pages. Tabulations for Y69, which used 769 hourly weather data measurements, are presented with the example in Appendix G.

In both listings column headings indicate wind speed classes. Row headings indicate wind directions.

Y68

METEOROLOGICAL INPUT DATA FOR THE ANNUAL SEASON

MIXING DEPTH = 970. METERS
AMBIENT TEMPERATURE = 289. DEGREES,KELVIN
AMBIENT PRESSURE = 981. MILLIBARS

STABILITY CLASS 1

	WINDSPEED CLASS					
WIND DIRECTION	1	2	3	4	5	6
N	.0064	.0064	.0112	.0032	.0016	.0000
NNE	.0032	.0000	.0016	.0000	.0000	.0000
NE	.0016	.0016	.0000	.0000	.0000	.0000
ENE	.0032	.0000	.0016	.0000	.0000	.0000
E	.0016	.0016	.0032	.0000	.0000	.0000
ESE	.0016	.0000	.0000	.0000	.0000	.0000
SE	.0048	.0048	.0000	.0000	.0000	.0000
SSE	.0080	.0016	.0016	.0032	.0000	.0000
S	.0064	.0032	.0000	.0000	.0000	.0000
SSW	.0032	.0048	.0032	.0000	.0000	.0000
SW	.0032	.0048	.0016	.0000	.0000	.0000
WSW	.0032	.0016	.0016	.0000	.0000	.0000
W	.0048	.0191	.0032	.0000	.0000	.0000
WNW	.0032	.0095	.0112	.0048	.0000	.0000
NW	.0143	.0653	.0717	.0653	.0430	.0095
NNW	.0095	.0287	.0414	.0350	.0143	.0000

Y68

METEOROLOGICAL INPUT DATA FOR THE ANNUAL SEASON

STABILITY CLASS 2

WIND DIRECTION	WINDSPEED CLASS 1	2	3	4	5	6
N	.0000	.0016	.0064	.0016	.0000	.0000
NNE	.0000	.0032	.0000	.0000	.0000	.0000
NE	.0016	.0000	.0000	.0000	.0000	.0000
ENE	.0000	.0000	.0000	.0000	.0000	.0000
E	.0016	.0016	.0000	.0000	.0000	.0000
ESE	.0000	.0016	.0000	.0000	.0000	.0000
SE	.0016	.0016	.0000	.0000	.0000	.0000
SSE	.0032	.0016	.0000	.0000	.0000	.0000
S	.0000	.0032	.0032	.0000	.0000	.0000
SSW	.0000	.0032	.0016	.0000	.0000	.0000
SW	.0032	.0016	.0032	.0016	.0016	.0000
WSW	.0032	.0000	.0000	.0000	.0016	.0016
W	.0000	.0000	.0016	.0000	.0000	.0000
WNW	.0032	.0016	.0000	.0000	.0000	.0000
NW	.0080	.0000	.0127	.0239	.0064	.0032
NNW	.0048	.0048	.0159	.0080	.0127	.0000

Y68

METEOROLOGICAL INPUT DATA FOR THE ANNUAL SEASON

STABILITY CLASS 3

	WINDSPEED CLASS					
WIND DIRECTION	1	2	3	4	5	6
N	.0000	.0000	.0000	.0048	.0032	.0000
NNE	.0000	.0000	.0000	.0000	.0000	.0000
NE	.0000	.0000	.0000	.0000	.0000	.0000
ENE	.0000	.0000	.0000	.0000	.0000	.0000
E	.0016	.0000	.0000	.0000	.0000	.0000
ESE	.0000	.0000	.0000	.0000	.0000	.0000
SE	.0000	.0000	.0000	.0000	.0000	.0000
SSE	.0000	.0000	.0000	.0000	.0000	.0000
S	.0000	.0000	.0000	.0016	.0000	.0000
SSW	.0000	.0000	.0016	.0000	.0000	.0000
SW	.0000	.0000	.0000	.0000	.0000	.0064
WSW	.0000	.0000	.0000	.0000	.0000	.0000
W	.0000	.0000	.0000	.0000	.0000	.0000
WNW	.0000	.0000	.0000	.0000	.0000	.0016
NW	.0000	.0000	.0016	.0016	.0032	.0000
NNW	.0000	.0000	.0064	.0112	.0064	.0016

Y68

METEORDLOGICAL INPUT DATA FOR THE ANNUAL SEASON

STABILITY CLASS 4

	WINDSPEED CLASS					
WIND DIRECTION	1	2	3	4	5	6
N	.0000	.0000	.0048	.0000	.0016	.0000
NNE	.0000	.0000	.0000	.0000	.0000	.0000
NE	.0016	.0000	.0000	.0000	.0000	.0000
ENE	.0000	.0000	.0000	.0000	.0000	.0000
E	.0000	.0000	.0016	.0000	.0000	.0000
ESE	.0000	.0000	.0000	.0000	.0000	.0000
SE	.0016	.0000	.0000	.0016	.0000	.0000
SSE	.0016	.0016	.0000	.0016	.0000	.0000
S	.0016	.0000	.0000	.0000	.0000	.0000
SSW	.0016	.0016	.0000	.0000	.0000	.0000
SW	.0000	.0000	.0000	.0000	.0000	.0000
WSW	.0016	.0000	.0000	.0000	.0000	.0000
W	.0000	.0000	.0016	.0000	.0000	.0000
WNW	.0000	.0000	.0000	.0016	.0000	.0000
NW	.0000	.0048	.0032	.0112	.0000	.0000
NNW	.0000	.0000	.0080	.0159	.0000	.0000

Y68

METEOROLOGICAL INPUT DATA FOR THE ANNUAL SEASON

STABILITY CLASS 5

	WINDSPEED CLASS					
WIND DIRECTION	1	2	3	4	5	6
N	.0000	.0000	.0016	.0000	.0000	.0000
NNE	.0000	.0000	.0000	.0000	.0000	.0000
NE	.0000	.0000	.0000	.0000	.0000	.0000
ENE	.0000	.0000	.0000	.0000	.0000	.0000
E	.0016	.0000	.0000	.0000	.0000	.0000
ESE	.0016	.0000	.0000	.0000	.0000	.0000
SE	.0000	.0000	.0000	.0000	.0000	.0000
SSE	.0016	.0000	.0000	.0000	.0000	.0000
S	.0573	.0000	.0000	.0000	.0000	.0000
SSW	.0000	.0000	.0000	.0000	.0000	.0000
SW	.0000	.0032	.0000	.0000	.0000	.0000
WSW	.0000	.0000	.0000	.0000	.0000	.0000
W	.0000	.0048	.0000	.0000	.0000	.0000
WNW	.0000	.0000	.0000	.0032	.0000	.0000
NW	.0016	.0016	.0064	.0048	.0048	.0000
NNW	.0032	.0016	.0048	.0080	.0143	.0000

Y68

METEOROLOGICAL INPUT DATA FOR THE ANNUAL SEASON

STABILITY CLASS 6

	WINDSPEED CLASS					
WIND DIRECTION	1	2	3	4	5	6
N	.0000	.0000	.0016	.0000	.0000	.0000
NNE	.0000	.0000	.0000	.0000	.0000	.0000
NE	.0000	.0000	.0000	.0000	.0000	.0000
ENE	.0016	.0000	.0000	.0000	.0000	.0000
E	.0000	.0016	.0000	.0000	.0000	.0000
ESE	.0000	.0000	.0000	.0000	.0000	.0000
SE	.0000	.0000	.0000	.0000	.0000	.0000
SSE	.0016	.0000	.0000	.0000	.0000	.0000
S	.0000	.0000	.0000	.0000	.0000	.0000
SSW	.0000	.0000	.0000	.0000	.0000	.0000
SW	.0000	.0000	.0000	.0000	.0000	.0000
WSW	.0000	.0000	.0000	.0000	.0000	.0000
W	.0000	.0000	.0000	.0000	.0000	.0000
WNW	.0000	.0000	.0000	.0000	.0000	.0000
NW	.0032	.0000	.0032	.0000	.0000	.0000
NNW	.0016	.0000	.0000	.0032	.0032	.0000

Y68

METEOROLOGICAL INPUT DATA FOR THE ANNUAL SEASON

STABILITY CLASS 7

	WINDSPEED CLASS					
WIND DIRECTION	1	2	3	4	5	6
N	.0016	.0000	.0000	.0000	.0000	.0000
NNE	.0000	.0000	.0000	.0000	.0000	.0000
NE	.0000	.0000	.0000	.0000	.0000	.0000
ENE	.0000	.0000	.0000	.0000	.0000	.0000
E	.0000	.0000	.0000	.0000	.0000	.0000
ESE	.0000	.0000	.0000	.0000	.0000	.0000
SE	.0000	.0000	.0000	.0000	.0000	.0000
SSE	.0000	.0000	.0000	.0000	.0000	.0000
S	.0000	.0016	.0000	.0000	.0000	.0000
SSW	.0000	.0016	.0000	.0000	.0000	.0000
SW	.0000	.0000	.0000	.0000	.0000	.0000
WSW	.0000	.0000	.0000	.0000	.0000	.0000
W	.0000	.0000	.0000	.0000	.0000	.0000
WNW	.0000	.0000	.0000	.0000	.0000	.0000
NW	.0000	.0000	.0000	.0000	.0000	.0000
NNW	.0000	.0000	.0000	.0000	.0000	.0000

APPENDIX D

EMISSION CALCULATIONS

Data required for the computation of the sulfur dioxide emission rate and stack gas exit velocity, includes:

1. MW output, MW.

2. Percent sulfur in the fuel. All S in the pulverized coal is assumed to combust to SO_2 and exhaust into the atmosphere. Predicted ground level concentrations will thus be more conservative than if incomplete sulfur combustion is assumed. Typically sulfur combustion for pulverized coal is 95% complete.

3. Percent excess air. These boiler units were operated at about 20% excess air.

4. Percent combustibles in the fuel. Fuel analyses indicated an average of 88% combustibles and 12% ash.

5. Pounds of steam produced per pound of coal. Inspection of boiler output and fuel usage showed 9.1 pounds of steam were produced per pound of coal.

6. Exhaust gas temperature, 270°F or 730°R.

7. Inner stack diameter at the top, d.

8. Heat content of the fuel, 12,000 Btu per pound.

The following assumptions are based on combustion experience:

1. For large units, 7000 pounds of steam are produced per MW.

2. Theoretical air requirements are 7.58 pounds of air/10,000 Btu released.

SO_2 emission rate, Q, in GPS:

$$\frac{MW}{hr} * \frac{7000 \text{ lb ST}}{MW} * \frac{1 \text{ lb coal}}{9.1 \text{ lb ST}} * \frac{\% \text{ S}}{100} * \frac{2 \text{ lb } SO_2}{1 \text{ lb S}} * .126 \frac{GPS}{PPH}$$

$$= 1.938 \text{ MW} * \%S \tag{28}$$

For a 100 MW/hr output using 2% S fuel:

$$Q = 1.938 \ (100)(2) = 387.7 \text{ GPS} \tag{29}$$

Stack gas exit velocity, V:

$$\frac{MW}{hr} * \frac{7000}{9.1} \left[\frac{12{,}000 \text{ Btu}}{\text{lb. coal}} * \frac{7.58 \text{ lb air}}{10{,}000} * 1.2 + .88\right] * \frac{4}{\pi d^2 \rho} *$$

$$\frac{1}{11811} \frac{MPS}{FPH} = 0.978 \frac{MW}{\rho d^2} \tag{30}$$

For example, if MW = 100

$$d = 10$$

$$\rho = 0.05444 \text{ lb/cf, air density at } 270°F$$

$$V = \frac{0.978 * 100}{.05444 * 10^2} = 17.97 \text{ MPS}$$

$$V = 58.9 \text{ FPS} \tag{31}$$

Table 15. Boiler Emission Data, Y68

	UNIT 1	UNIT 2	UNIT 3	UNIT 4	ALL UNITS
Ave SO_2 Emission Rate Grams Per Second	970.3	983.1	791.8	0.0	2745.2
Arith Stand Dev, GPS	387.7	578.3	893.9	0.0	1320.8
Geom Stand Dev, GPS	1.5	1.7	2.5	0.0	1.6
Geom Mean, GPS	901.0	847.4	525.0	0.0	2473.8
Q Max, GPS	2721.8	2099.4	2965.8	0.0	6577.2
Pounds Per Hour	7700.6	7802.7	6283.9	0.0	21787.2
Arith Stand Dev, PPH	3076.8	4590.0	7094.1	0.0	10482.3
Ave Linear Velocity At 730.0 Degrees R					
Meters Per Second	17.8	24.5	18.1	0.0	
V Max, MPS	51.8	29.0	22.4	0.0	21.1
Feet Per Minute	3504.4	4827.9	3545.9	0.0	
Stack Diameter					
Meters	4.9	4.6	6.4	6.4	11.3
Feet	16.0	15.0	21.0	21.0	36.9

Number of Hourly Measurements or Ambient Samples Used 628

Total Operating Hours for UNIT 1 618
Total Operating Hours for UNIT 2 522
Total Operating Hours for UNIT 3 309
Total Operating Hours for UNIT 4 0
Starting Date 01 04 68 07 Ending Date 12 31 68 24

Table 16. Boiler Emission Data, Y69

	UNIT 1	UNIT 2	UNIT 3	UNIT 4	ALL UNITS
Ave SO_2 Emission Rate					
Grams Per Second	812.8	739.4	895.5	184.5	2632.3
Arith Stand Dev, GPS	278.1	543.6	781.4	441.8	1225.8
Geom Stand Dev, GPS	1.4	1.9	2.1	4.0	1.6
Geom Mean, GPS	769.1	595.8	674.8	71.1	2386.2
Q Max, GPS	2721.8	2163.3	2965.8	1512.0	6309.7
Pounds Per Hour	6451.0	5868.5	7107.5	1464.3	20891.3
Arith Stand Dev, PPH	2207.1	4314.1	6201.7	3506.0	9728.9
Ave Linear Velocity At 730.0 Degrees R					
Meters Per Second	17.7	23.8	18.0	18.7	
V Max, MPS	51.8	59.4	23.2	21.6	22.4
Feet Per Minute	3492.3	4687.0	3536.6	3711.9	
Stack Diameter					
Meters	4.9	4.6	6.4	6.4	11.3
Feet	16.0	15.0	21.0	21.0	36.9

Number of Hourly Measurements or Ambient Samples Used 769

Total Operating Hours for UNIT 1 764
Total Operating Hours for UNIT 2 590
Total Operating Hours for UNIT 3 488
Total Operating Hours for UNIT 4 119
Starting Date 10 01 68 12 Ending Date 08 20 69 15

Table 17. Frequency Distribution of Total Powerhouse Emission Output

Emission Range GPS	Frequency		Cumulative Frequency	
	Y68	Y69	Y68	Y69
0-500	0.5	0.1	0.5	0.1
500-1000	3.4	5.9	3.9	6.0
1000-1500	10.5	13.1	14.4	19.1
1500-2000	12.7	16.1	27.1	35.2
2000-2500	25.8	16.7	52.9	51.9
2500-3000	11.9	12.8	64.8	64.7
3000-4000	20.2	18.9	85.0	83.6
4000-5000	5.3	11.5	90.3	95.1
5000-6000	5.8	3.2	96.1	98.3
6000-7000	3.9	1.7	100.0	100.0

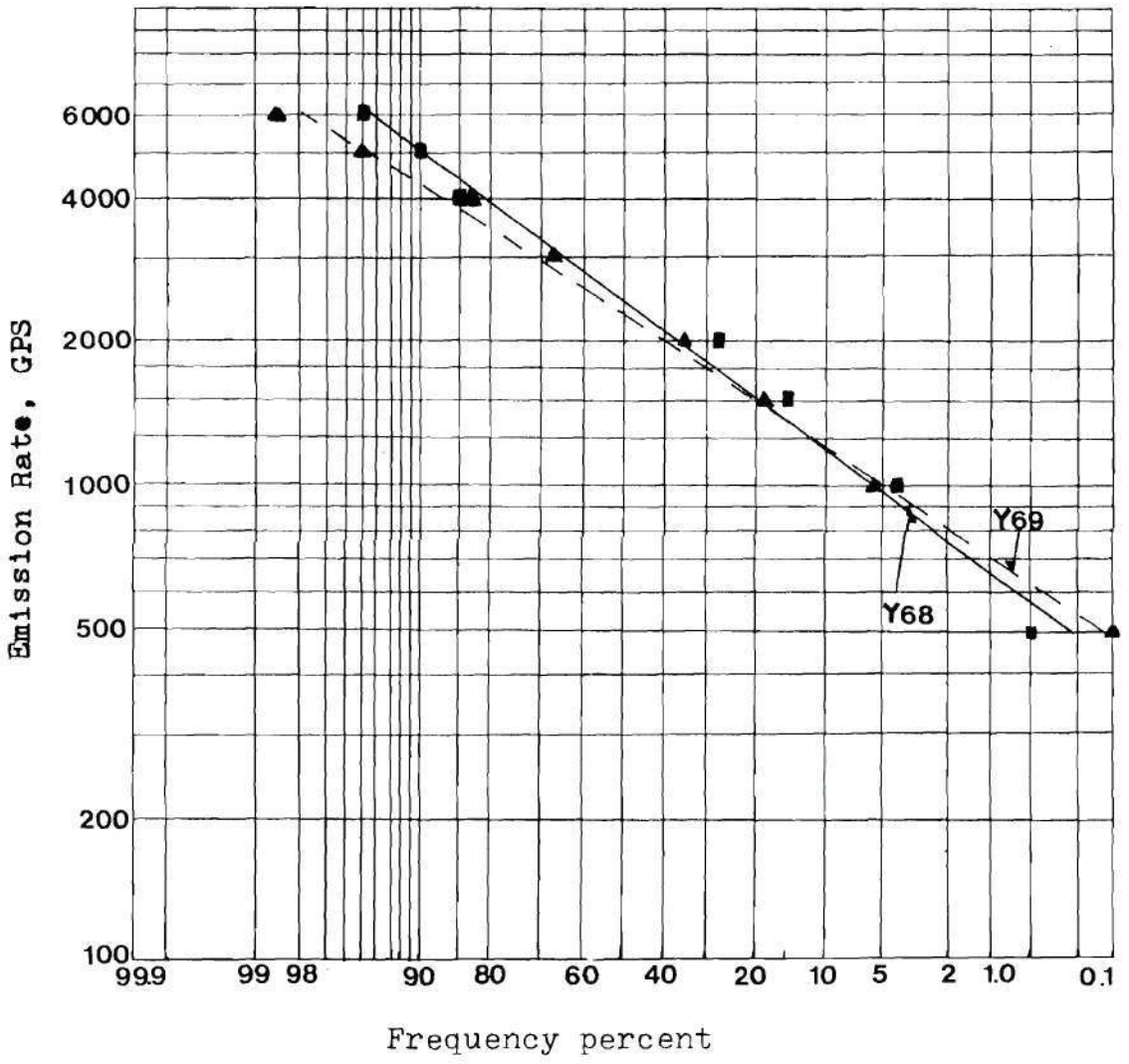

Figure 11. Cumulative Frequency of Total Power House Emissions Output Y68, Y69.

APPENDIX E

NOMENCLATURE

AM	arithmetic mean
ASD	arithmetic standard deviation
AQDM	Air Quality Display Model
d	diameter
GSD	geometric standard deviation
GPS	grams per second
h	effective stack height, m
Δh	plume rise
h_{eff}	effective stack height, m
$\Delta h(x)$	plume rise as a function of distance
L	height of mixing layer or stability class index
MPS	meters per second
MW	megawatts
n	empirical constant
NA	not available
PALSEM	Point, Area, and Line Source Emission Model
PC	pulverized coal
PPH	pounds per hour
ppm	parts per million
q	line source strength, µg/m.sec.
Q	emission rate, µg/sec, TPH, GPS

$\bar{Q}$	average emission rate
Q_H	heat flux
$\bar{Q}_m$	geometric mean emission rate
Q_{max}	maximum emission rate
R	relative concentration function
s	stability class index
S	length of line source
ST	steam
T	pollutant half-life, hours
TPH	tons per hour
TR	sampling trailer
u	wind speed, MPS
V	exhaust gas velocity
$V(\Delta h)$	wind velocity as a function of plume rise
V_o	wind velocity at Z_o
x	downwind distance
X_L	downwind distance
z	vertical height
Z_o	anemometer height
χ	concentration, $\mu g/m^3$
χ_n	non-reactive pollutant concentration, $\mu g/m^3$
χ_o	concentration, $\mu g/m^3$
χ_r	reactive pollutant concentration, $\mu g/m^3$
σ_e	GSD of emissions
σ_m	GSD due to meteorology

σ_T GSD due to emissions and meteorology

σ_z vertical Gaussian standard deviation, m

θ_1, θ_2 angle between receptor and centerline of sector

APPENDIX F

CONVERSION FACTORS

GPS/0.126 = PPH

GPS/10.5 = TPD

MPS/0.3048 = FPS

Km/1.609 = Mi

MPS/0.447 = Mi/Hr

$$\frac{\mu g/m^3}{21957.7} * \frac{T_a}{P_a M_a} = ppm$$

T_a = absolute gas temperature, °R

= ambient temperature +460.16°F

P_a = absolute gas pressure, Atm

M_a = molecular weight

For SO_2 at 70°F, 1 atm:

79.6 $\mu g/m^3$ = 0.03 ppm

26.5 $\mu g/m^3$ = 0.01 ppm

For SO_2 at 289°R, 981 mb

$$\frac{\mu g}{m^3} = ppm \left(21957.7 * \frac{981}{1013} * \frac{64.06}{520.2}\right) = 2618.6 * ppm$$

or

$$1 \text{ ppm} = 2618.6 \ \mu g/m^3$$

APPENDIX G

EXAMPLE PALSEM OUTPUT

In this run the Briggs' plume rise equation with no background concentration was used to model Y69. Locations of TR 5 and TR 6 correspond to receptor sites 15 and 31, respectively.

```
PALSEM SO2 PREDICTION FOR FOSSIL FUEL POWER PLANT Y69 BRIGGS PLUME RISE
NSORCE =    4
IFLAG =  0
IPUNCH =  1
NSEL5 =  0
NSEL12 =  1
NPOLUT =  1
NSO2 =   0
NPART =   0
ICONS =    0    0    0    0    0
ICONP =    0    0    0    0    0
ISTATS =   15   31    0    0    0    0
           0    0    0    0    0    0
ISTATP =   0    0    0    0    0    0
           0    0    0    0    0    0
INCRX,Y,Z =   2  16   1
DELTAX,Y,Z =     .000     .000     .000
IADD =  0
XRECEP =      .000      .000      .000      .000      .000      .000
              .000      .000      .000      .000      .000      .000
              .000      .000      .000      .000      .000      .000
              .000      .000      .000      .000      .000      .000
              .000      .000      .000      .000      .000      .000
              .000      .000      .000      .000      .000      .000
BACKGR =     .000     .000
SO2CAL =     .0000   1.0000
PARCAL =     .0000   1.0000
SGOS = 2.60 1.79  .00  .00  .00  .00  .00  .00  .00  .00  .00  .00
SGOP =  .00  .00  .00  .00  .00  .00  .00  .00  .00  .00  .00  .00
SO2AVG =   1.00   3.00  24.00
PARAVG =    .00    .00    .00
RBASE =      .000      .000      .000
RSHGT =     .000
NSEG =    7
NPLREQ =   5
ICROSS =  0
ICOORD =  2
XCOORD =     5.710     7.320      .000      .000      .000      .000      .000      .000      .000
NSORGN =  0
ZO =     .0
HALF =  10000.0  10000.0
WSPD =      .600
NSAZ =     0
NSSC =     0
NSSP =     0
SUM =    1.60     .00
TA =  289.00
PA =  981.00
DPTHMX =   970.00
DMXE =       100.
FREQM1 =    .400
NSC =  7
```

PALSEM SO2 PREDICTION FOR FOSSIL FUEL POWER PLANT Y69 BRIGGS PLUME RISE

POINT AND AREA SOURCE DATA RMHGT = .000

SOURCE NUMBER	SOURCE LOCATION (KILOMETERS) EASTWARD	NORTHWARD	HEIGHT	SOURCE AREA SQUARE KILOMETERS	ANNUAL SOURCE EMISSION RATE (TONS/DAY) SO2	PART	STACK DATA HT (M)	DIAM (M)	VEL (M/SEC)	TEMP (DEG.K)	PERCENT INCREASE
1	.00	.00	.000	.000	77.409	.000	91.4	4.9	17.7	405.	.0
2	.00	.00	.000	.000	70.419	.000	106.7	4.6	23.8	405.	.0
3	.00	.00	.000	.000	85.286	.000	152.4	6.4	18.0	405.	.0
4	.00	.00	.000	.000	17.571	.000	152.4	6.4	18.7	405.	.0

PALSEM 502 PREDICTION FOR FOSSIL FUEL POWER PLANT Y69 BRIGGS PLUME RISE

METEOROLOGICAL INPUT DATA FOR THE ANNUAL SEASON

MIXING DEPTH = 970. METERS
AMBIENT TEMPERATURE = 289. DEGREES,KELVIN
AMBIENT PRESSURE = 981. MILLIBARS

STABILITY CLASS 1

	WINDSPEED CLASS					
WIND DIRECTION	1	2	3	4	5	6
N	.0117	.0104	.0208	.0026	.0013	.0000
NNE	.0052	.0026	.0026	.0013	.0000	.0000
NE	.0013	.0026	.0013	.0000	.0000	.0000
ENE	.0013	.0013	.0052	.0000	.0000	.0000
E	.0013	.0000	.0000	.0000	.0000	.0000
ESE	.0013	.0000	.0000	.0000	.0000	.0000
SE	.0065	.0026	.0013	.0000	.0000	.0000
SSE	.0052	.0013	.0013	.0026	.0000	.0000
S	.0078	.0013	.0039	.0013	.0000	.0000
SSW	.0039	.0026	.0039	.0000	.0000	.0000
SW	.0130	.0039	.0026	.0013	.0000	.0000
WSW	.0026	.0078	.0039	.0000	.0000	.0000
W	.0065	.0104	.0039	.0000	.0000	.0000
WNW	.0065	.0052	.0052	.0026	.0000	.0000
NW	.0091	.0234	.0312	.0234	.0013	.0000
NNW	.0091	.0299	.0520	.0377	.0208	.0065

PALSEM SO2 PREDICTION FOR FOSSIL FUEL POWER PLANT Y69 BRIGGS PLUME RISE

METEOROLOGICAL INPUT DATA FOR THE ANNUAL SEASON

STABILITY CLASS 2

WIND DIRECTION	WINDSPEED CLASS 1	2	3	4	5	6
N	.0000	.0039	.0052	.0013	.0000	.0000
NNE	.0000	.0013	.0013	.0013	.0000	.0000
NE	.0000	.0000	.0000	.0000	.0000	.0000
ENE	.0000	.0000	.0026	.0000	.0000	.0000
E	.0000	.0000	.0000	.0000	.0000	.0000
ESE	.0000	.0000	.0000	.0013	.0000	.0000
SE	.0000	.0000	.0052	.0013	.0000	.0000
SSE	.0000	.0000	.0000	.0000	.0000	.0000
S	.0013	.0000	.0026	.0000	.0000	.0000
SSW	.0000	.0000	.0000	.0000	.0000	.0000
SW	.0000	.0000	.0026	.0013	.0013	.0000
WSW	.0013	.0000	.0000	.0000	.0013	.0013
W	.0000	.0000	.0000	.0000	.0000	.0000
WNW	.0026	.0000	.0000	.0000	.0000	.0000
NW	.0000	.0013	.0013	.0117	.0013	.0000
NNW	.0039	.0026	.0182	.0195	.0104	.0013

PALSEM SO2 PREDICTION FOR FOSSIL FUEL POWER PLANT Y69 BRIGGS PLUME RISE

METEOROLOGICAL INPUT DATA FOR THE ANNUAL SEASON

STABILITY CLASS 3

	WINDSPEED CLASS					
WIND DIRECTION	1	2	3	4	5	6
N	.0000	.0000	.0013	.0039	.0026	.0000
NNE	.0000	.0013	.0000	.0000	.0000	.0000
NE	.0000	.0000	.0000	.0013	.0000	.0000
ENE	.0013	.0000	.0000	.0000	.0000	.0000
E	.0013	.0000	.0000	.0013	.0000	.0000
ESE	.0000	.0013	.0000	.0039	.0000	.0000
SE	.0000	.0000	.0026	.0013	.0000	.0000
SSE	.0000	.0000	.0013	.0013	.0000	.0000
S	.0000	.0039	.0013	.0013	.0000	.0000
SSW	.0000	.0000	.0000	.0013	.0000	.0000
SW	.0000	.0000	.0000	.0000	.0000	.0052
WSW	.0000	.0000	.0000	.0000	.0000	.0000
W	.0000	.0000	.0000	.0039	.0000	.0000
WNW	.0000	.0000	.0000	.0000	.0000	.0013
NW	.0000	.0013	.0065	.0078	.0026	.0013
NNW	.0000	.0000	.0130	.0299	.0156	.0026

PALSEM SO2 PREDICTION FOR FOSSIL FUEL POWER PLANT Y69 BRIGGS PLUME RISE

METEOROLOGICAL INPUT DATA FOR THE ANNUAL SEASON

STABILITY CLASS 4

	WINDSPEED CLASS					
WIND DIRECTION	1	2	3	4	5	6
N	.0000	.0000	.0000	.0065	.0039	.0000
NNE	.0000	.0000	.0000	.0000	.0000	.0000
NE	.0000	.0000	.0000	.0013	.0000	.0000
ENE	.0000	.0000	.0000	.0000	.0000	.0000
E	.0000	.0013	.0000	.0026	.0000	.0000
ESE	.0000	.0000	.0000	.0013	.0013	.0000
SE	.0000	.0000	.0013	.0000	.0000	.0000
SSE	.0000	.0000	.0039	.0000	.0000	.0000
S	.0000	.0000	.0000	.0026	.0013	.0000
SSW	.0000	.0000	.0026	.0000	.0000	.0000
SW	.0000	.0000	.0000	.0000	.0000	.0000
WSW	.0000	.0000	.0000	.0000	.0039	.0000
W	.0000	.0000	.0000	.0000	.0000	.0000
WNW	.0000	.0000	.0000	.0000	.0000	.0000
NW	.0000	.0000	.0039	.0130	.0052	.0000
NNW	.0013	.0000	.0065	.0312	.0117	.0013

PALSEM SO2 PREDICTION FOR FOSSIL FUEL POWER PLANT Y69 BRIGGS PLUME RISE

METEOROLOGICAL INPUT DATA FOR THE ANNUAL SEASON

STABILITY CLASS 5

	WINDSPEED CLASS					
WIND DIRECTION	1	2	3	4	5	6
N	.0000	.0000	.0052	.0078	.0026	.0000
NNE	.0000	.0013	.0026	.0000	.0000	.0000
NE	.0000	.0013	.0026	.0000	.0000	.0000
ENE	.0000	.0000	.0000	.0000	.0000	.0000
E	.0000	.0013	.0000	.0013	.0000	.0000
ESE	.0026	.0000	.0000	.0000	.0000	.0000
SE	.0000	.0013	.0013	.0000	.0000	.0000
SSE	.0000	.0013	.0013	.0013	.0000	.0000
S	.0624	.0013	.0039	.0026	.0000	.0000
SSW	.0000	.0000	.0000	.0000	.0000	.0000
SW	.0000	.0000	.0000	.0000	.0000	.0000
WSW	.0013	.0000	.0000	.0000	.0013	.0000
W	.0000	.0000	.0000	.0000	.0000	.0000
WNW	.0000	.0000	.0000	.0039	.0000	.0000
NW	.0000	.0000	.0000	.0104	.0039	.0000
NNW	.0000	.0013	.0026	.0234	.0156	.0000

PALSEM SO2 PREDICTION FOR FOSSIL FUEL POWER PLANT Y69 BRIGGS PLUME RISE

METEOROLOGICAL INPUT DATA FOR THE ANNUAL SEASON

STABILITY CLASS 6

	WINDSPEED CLASS					
WIND DIRECTION	1	2	3	4	5	6
N	.0000	.0000	.0013	.0052	.0000	.0000
NNE	.0000	.0000	.0052	.0000	.0000	.0000
NE	.0013	.0013	.0013	.0000	.0000	.0000
ENE	.0000	.0000	.0000	.0013	.0000	.0000
E	.0000	.0013	.0000	.0013	.0000	.0000
ESE	.0000	.0000	.0013	.0000	.0000	.0000
SE	.0000	.0000	.0000	.0000	.0000	.0000
SSE	.0000	.0013	.0000	.0000	.0000	.0000
S	.0000	.0013	.0026	.0000	.0000	.0000
SSW	.0000	.0013	.0000	.0000	.0000	.0000
SW	.0000	.0000	.0000	.0000	.0013	.0000
WSW	.0000	.0000	.0000	.0000	.0000	.0000
W	.0000	.0000	.0000	.0000	.0000	.0000
WNW	.0000	.0000	.0000	.0000	.0000	.0000
NW	.0000	.0013	.0000	.0000	.0000	.0000
NNW	.0000	.0000	.0000	.0078	.0000	.0000

PALSEM SO2 PREDICTION FOR FOSSIL FUEL POWER PLANT Y69 BRIGGS PLUME RISE

METEOROLOGICAL INPUT DATA FOR THE ANNUAL SEASON

STABILITY CLASS 7

	WINDSPEED CLASS					
WIND DIRECTION	1	2	3	4	5	6
N	.0000	.0000	.0000	.0000	.0000	.0000
NNE	.0000	.0000	.0000	.0000	.0000	.0000
NE	.0000	.0000	.0000	.0000	.0000	.0000
ENE	.0000	.0000	.0000	.0000	.0000	.0000
E	.0000	.0000	.0000	.0000	.0000	.0000
ESE	.0000	.0013	.0000	.0000	.0000	.0000
SE	.0000	.0000	.0000	.0000	.0000	.0000
SSE	.0000	.0000	.0000	.0000	.0000	.0000
S	.0000	.0000	.0000	.0000	.0000	.0000
SSW	.0000	.0000	.0000	.0000	.0000	.0000
SW	.0000	.0000	.0000	.0000	.0000	.0000
WSW	.0000	.0000	.0000	.0000	.0000	.0000
W	.0000	.0000	.0000	.0000	.0000	.0000
WNW	.0000	.0000	.0000	.0000	.0000	.0000
NW	.0000	.0000	.0000	.0026	.0013	.0000
NNW	.0000	.0000	.0000	.0013	.0013	.0013

PALSEM SO2 PREDICTION FOR FOSSIL FUEL POWER PLANT Y69 BRIGGS PLUME RISE

RECEPTOR INFORMATION FOR STATISTICAL OUTPUT

SO2		PARTICULATES	
SELECTED RECEPTOR NO.	STANDARD GEOMETRIC DEVIATION (24 HR. AVERAGING TIME)	SELECTED RECEPTOR NO.	STANDARD GEOMETRIC DEVIATION (24 HR. AVERAGING TIME)
15	2.00	0	.00
31	1.79	0	.00
0	.00	0	.00
0	.00	0	.00
0	.00	0	.00
0	.00	0	.00
0	.00	0	.00
0	.00	0	.00
0	.00	0	.00
0	.00	0	.00
0	.00	0	.00
0	.00	0	.00

PALSEM SO2 PREDICTION FOR FOSSIL FUEL POWER PLANT Y69 BRIGGS PLUME RISE

INPUT REGRESSION PARAMETERS ARE\

POLLUTANT	Y-INTERCEPT	SLOPE
SO2	.0	1.0000

RMHGT = .000

RECEPTOR CONCENTRATION DATA

RECEPTOR NUMBER	RECEPTOR LOCATION (KILOMETERS) EAST	NORTH	HEIGHT	EXPECTED ARITHMETIC MEAN (MICROGRAMS/CU. METER) SO2	PARTICULATES
1	5.710	.000	.000	5.13	.00
2	5.275	2.185	.000	3.79	.00
3	4.038	4.038	.000	4.02	.00
4	2.185	5.275	.000	1.90	.00
5	.000	5.710	.000	3.47	.00
6	-2.185	5.275	.000	1.67	.00
7	-4.038	4.038	.000	3.84	.00
8	-5.275	2.185	.000	1.57	.00
9	-5.710	.000	.000	.40	.00
10	-5.275	-2.185	.000	2.09	.00
11	-4.038	-4.038	.000	1.46	.00
12	-2.185	-5.275	.000	2.80	.00
13	.000	-5.710	.000	13.36	.00
14	2.185	-5.275	.000	54.10	.00
15	4.038	-4.038	.000	24.94	.00
16	5.275	-2.185	.000	3.19	.00
17	7.320	.000	.000	3.98	.00
18	6.763	2.801	.000	3.04	.00
19	5.176	5.176	.000	3.00	.00
20	2.801	6.763	.000	1.49	.00
21	.000	7.320	.000	3.06	.00
22	-2.801	6.763	.000	1.35	.00
23	-5.176	5.176	.000	3.00	.00
24	-6.763	2.801	.000	1.34	.00
25	-7.320	.000	.000	.36	.00
26	-6.763	-2.801	.000	1.61	.00
27	-5.176	-5.176	.000	1.16	.00
28	-2.801	-6.763	.000	2.35	.00
29	.000	-7.320	.000	10.71	.00
30	2.801	-6.763	.000	42.71	.00

PALSEM SO2 PREDICTION FOR FOSSIL FUEL POWER PLANT Y69 BRIGGS PLUME RISE

RMHGT = .000

RECEPTOR NUMBER	RECEPTOR LOCATION (KILOMETERS) EAST	NORTH	HEIGHT	EXPECTED ARITHMETIC MEAN (MICROGRAMS/CU. METER) SO2	PARTICULATES
31	5.176	-5.176	.000	19.91	.00
32	6.763	-2.801	.000	2.47	.00

SITE	HOURLY SO2 DISTRIBUTION							MET.DISTRIBUTION		MET.+EMISSION DISTRIBUTION		
	0	0- 50	50- 100	100- 200	200- 400	400- 800	800-9999	SG	1 HR.MAX	SG	1 HR.MAX	3.HR.MAX
1	98.18	.00	.00	.39	1.43	.00	.00	.00	.0	.00	.0	.0
2	98.18	.00	.39	.65	.78	.00	.00	6.06	672.4	6.43	1089.2	549.1
3	98.18	.00	.00	1.17	.65	.00	.00	.00	.0	.00	.0	.0
4	98.96	.26	.00	.39	.39	.00	.00	8.99	798.4	9.44	958.8	451.6
5	98.05	.26	.13	.91	.65	.00	.00	5.34	679.4	5.70	862.0	442.2
6	98.83	.39	.00	.39	.39	.00	.00	8.99	798.4	9.44	958.8	444.5
7	98.44	.13	.00	.26	1.17	.00	.00	14.70	2749.7	15.31	3195.0	1416.3
8	99.09	.13	.13	.26	.39	.00	.00	9.21	824.0	9.68	987.6	452.9
9	99.48	.39	.00	.00	.13	.00	.00	.00	.0	.00	.0	.0
10	99.09	.00	.00	.52	.39	.00	.00	.00	.0	.00	.0	.0
11	99.35	.13	.00	.13	.39	.00	.00	22.96	1659.9	23.77	1886.5	793.5
12	98.83	.00	.00	.65	.39	.13	.00	.00	.0	.00	.0	.0
13	93.83	.65	.52	2.47	2.34	.39	.00	3.58	728.9	3.69	992.4	589.3
14	68.92	3.77	4.03	12.35	10.06	.26	.00	2.18	551.4	2.49	891.7	635.2
15	86.35	1.69	.65	7.02	4.16	.13	.00	2.58	534.6	2.88	802.1	527.0
16	98.57	.00	.00	.91	.52	.00	.00	.00	.0	.00	.0	.0
17	98.18	.00	.00	.78	1.04	.00	.00	.00	.0	.00	.0	.0
18	98.18	.00	.65	.39	.78	.00	.00	4.29	505.1	4.62	663.1	345.6
19	98.18	.00	.26	.91	.65	.00	.00	7.69	1528.7	8.32	1613.6	754.0
20	98.96	.26	.00	.52	.26	.00	.00	6.59	539.7	6.98	667.3	318.9
21	98.05	.26	.26	.91	.52	.00	.00	4.78	572.5	5.13	738.1	380.1
22	98.83	.39	.26	.26	.26	.00	.00	6.74	555.4	7.14	685.1	322.3
23	98.44	.13	.00	.39	1.04	.00	.00	10.94	1771.8	11.46	2096.5	949.1
24	99.09	.13	.13	.65	.00	.00	.00	10.64	1011.6	11.35	1197.8	526.3
25	99.48	.39	.00	.13	.00	.00	.00	.00	.0	.00	.0	.0
26	99.09	.00	.00	.52	.39	.00	.00	.00	.0	.00	.0	.0
27	99.35	.13	.00	.26	.26	.00	.00	11.20	744.4	11.72	879.5	394.1
28	98.83	.00	.13	.52	.52	.00	.00	11.76	1628.5	12.30	1917.7	852.0
29	93.83	.65	.78	2.86	2.08	.00	.00	3.56	722.8	3.88	985.0	569.9
30	68.92	3.77	8.97	11.96	6.37	.00	.00	2.18	550.8	2.49	891.0	616.9
31	86.35	1.69	3.12	5.59	3.25	.00	.00	2.71	607.8	3.01	895.0	564.7
32	98.57	.00	.26	.65	.52	.00	.00	7.49	1007.0	7.91	1229.0	579.6

PALSEM SO2 PREDICTION FOR FOSSIL FUEL POWER PLANT Y69 BRIGGS PLUME RISE

STATISTICAL DATA FOR SELECTED RECEPTORS

ANNUAL SO2

MICROGRAMS PER CUBIC METER

AVERAGING TIME 1. HOURS

RECEPTOR NUMBER	EXPECTED ARITHMETIC MEAN	EXPECTED GEOMETRIC MEAN	EXPECTED MAXIMUM CONCENTRATION	STANDARD GEOMETRIC DEVIATION
15	25.	17.	457.	2.36
31	20.	15.	241.	2.06

PALSEM SO2 PREDICTION FOR FOSSIL FUEL POWER PLANT Y69 BRIGGS PLUME RISE

STATISTICAL DATA FOR SELECTED RECEPTORS

ANNUAL SO2

MICROGRAMS PER CUBIC METER

AVERAGING TIME 3. HOURS

RECEPTOR NUMBER	EXPECTED ARITHMETIC MEAN	EXPECTED GEOMETRIC MEAN	EXPECTED MAXIMUM CONCENTRATION	STANDARD GEOMETRIC DEVIATION
15	25.	18.	311.	2.24
31	20.	16.	173.	1.97

PALSEM SO2 PREDICTION FOR FOSSIL FUEL POWER PLANT Y69 BRIGGS PLUME RISE

STATISTICAL DATA FOR SELECTED RECEPTORS

ANNUAL SO2

MICROGRAMS PER CUBIC METER

AVERAGING TIME 24. HOURS

RECEPTOR NUMBER	EXPECTED ARITHMETIC MEAN	EXPECTED GEOMETRIC MEAN	EXPECTED MAXIMUM CONCENTRATION	STANDARD GEOMETRIC DEVIATION
15	25.	20.	150.	2.00
31	20.	17.	93.	1.79

PALSEM SO2 PREDICTION FOR FOSSIL FUEL POWER PLANT Y69 BRIGGS PLUME RISE

SOURCE CONTRIBUTIONS TO FIVE MAXIMUM RECEPTORS

ANNUAL SO2

MICROGRAMS PER CUBIC METER

SOURCE	RECEPTOR 14	RECEPTOR 30	RECEPTOR 15	RECEPTOR 31	RECEPTOR 13
1	34.83 %	34.45 %	34.20 %	34.12 %	33.81 %
	18.8395	14.7163	8.5270	6.7947	4.5187
2	29.19 %	28.89 %	28.89 %	28.75 %	28.81 %
	15.7918	12.3382	7.2034	5.7261	3.8500
3	29.86 %	30.41 %	30.62 %	30.80 %	31.00 %
	16.1511	12.9891	7.6365	6.1333	4.1433
4	6.13 %	6.25 %	6.29 %	6.33 %	6.37 %
	3.3147	2.6689	1.5689	1.2608	.8513
BACK-GROUND	.00 %	.00 %	.00 %	.00 %	.00 %
	0.	0.	0.	0.	0.
TOTAL	100.0 %	100.0 %	100.0 %	100.0 %	100.0 %
	54.0971	42.7125	24.9358	19.9149	13.3632

DIRECTION DISTRIBUTIONS FOR HOURLY CONCENTRATIONS OF SO2

SITE =	14	30	15	31	13
N	.000	.000	.000	.000	137.045
NNE	.000	.000	.000	.000	.000
NE	.000	.000	.000	.000	.000
ENE	.000	.000	.000	.000	.000
E	.000	.000	.000	.000	.000
ESE	.000	.000	.000	.000	.000
SE	.000	.000	.000	.000	.000
SSE	.000	.000	.000	.000	.000
S	.000	.000	.000	.000	.000
SSW	.000	.000	.000	.000	.000
SW	.000	.000	.000	.000	.000
WSW	.000	.000	.000	.000	.000
W	.000	.000	.000	.000	.000
WNW	.000	.000	.000	.000	.000
NW	.000	.000	151.007	120.601	.000
NNW	142.473	112.490	.000	.000	.000

```
END OF FILE ENCOUNTERED -- TERMINATE RUN.

NORMAL EXIT.  EXECUTION TIME:        13463 MLSEC.
$FIN


RUNID: PALS4     ACCT: 181A0116       PROJECT: JUSTUS-C-G
TIME:     TOTAL: 00:00:19.214
          CPU:   00:00:13.463      I/O:  00:00:03.699
          CC/ER: 00:00:02.051      WAIT: 00:00:00.000
IMAGES  READ:    141       PAGES:  21
START:    13:49:53 JUL 28,1975    FIN:  13:50:27 JUL 28,1975
```

BIBLIOGRAPHY

1. Davis Sulfur Dioxide Monitor Instruction Book, Models 70A1 and 70A2, Davis Instruments, Newark, New Jersey, 1968.

2. Justus, C. G.: "The Point, Area, and Line Source Emission Model," School of Aerospace Engineering, Georgia Institute of Technology, 1975.

3. Koch, Robert C. and Scott D. Thayer: Validation and Sensitivity Analysis of the Gaussian Plume Multiple Source Diffusion Model, EPA Contract No. CPA 70-94, Report No. APTD-0935, November, 1971.

4. Larsen, Ralph I.: A Mathematical Model for Relating Air Quality Measurements to Air Quality Standards. Environmental Protection Agency, Office of Air Programs, Research Triangle Park, North Carolina, November, 1971.

5. Martin, Delance O. and Tikvart, Joseph A., June, 1968: "A General Atmospheric Diffusion Model for Estimating the Effects on Air Quality of One or More Sources," APCA Paper, pages 68-148.

6. McNair, Larry D.: "Air Quality Program Study, PHB," Southern Services, Inc., Research Department, Birmingham, Alabama, November, 1973.

7. Palmer, H. F., C. J. Nelson, and C. E. Rodes: "Performance Characteristics of Instrumental Methods for Monitoring Sulfur Dioxide," Paper No. 69-89, APCA Annual Meeting, 1969.

8. Pasquill, Frank: Atmospheric Diffusion, D. Van Nostrand Company, LTD, London, 1962.

9. Slade, David H., Editor: "Meteorology and Atomic Energy 1968," U. S. Atomic Energy Commission, TID 24190, July, 1968.

10. TRW Systems Group: Air Quality Display Model, EPA Contract No. PH-22-68-60, November, 1969.

11. Briggs, G. A.: "Plume Rise: A Critical Survey," Air Resources Atmospheric Turbulence and Diffusion Laboratory, Oak Ridge, Tenn., U. S. Atomic Energy Commission, Division of Technical Information, USAEC Critical Review Series, Publication Number TID 25075, 1969.

12. Holland, J. Z.: "A Meteorological Survey of the Oak Ridge Area," Atomic Energy Commission Report ORO-99, Washington, D. C., 1953.